ARL-STRUC-NOTE-486

AR-002-948

DEPARTMENT OF DEFENCE

DEFENCE SCIENCE AND TECHNOLOGY ORGANISATION

AERONAUTICAL RESEARCH LABORATORIES

MELBOURNE, VICTORIA

STRUCTURES NOTE 486

IMPROVING THE FATIGUE PERFORMANCE OF THICK ALUMINIUM ALLOY BOLTED JOINTS BY HOLE COLD-EXPANSION AND THE USE OF INTERFERENCE-FIT STEEL BUSHES

by

J. Y. Mann, G. W. Revill and W. F. Lupson

APRIL 1983

COPY No

AR-002-948

DEPARTMENT OF DEFENCE
DEFENCE SCIENCE AND TECHNOLOGY ORGANISATION
AERONAUTICAL RESEARCH LABORATORIES

STRUCTURES NOTE 486

IMPROVING THE FATIGUE PERFORMANCE OF THICK ALUMINIUM ALLOY BOLTED JOINTS BY HOLE COLD-EXPANSION AND THE USE OF INTERFERENCE-FIT STEEL BUSHES

by

J. Y. Mann, G. W. Revill and W. F. Lupson

SUMMARY

Fatigue tests under a flight-by-flight loading sequence have been carried out on small bolted joint specimens of 23 mm thickness representing part of the spar rear flange/skin attachment in Mirage III aircraft.

The investigation has shown that by cold-expanding the bolt holes to take standard oversize bolts, or by installing interference-fit bushes, the fatigue life can be more than doubled compared with the use of standard close-fit bolts in reamed holes. No significant differences were found between the fatigue lives of specimens embodying low-alloy steel or stainless steel bushes.

When small-sized residual fatigue cracks are present, hole cold-expansion may be a suitable process for extending the fatigue life. The use of interference-fit bushes is not likely to be an effective method for extending the fatigue lives when large-size residual cracks are present. However, if such cracks can be machined out, the incorporation of large-size interference-fit bushes has the greater potential for providing not only significant extensions in life but also significantly longer lives than the original design detail.

POSTAL ADDRESS: Director, Aeronautical Research Laboratories,
Box 4331, P.O., Melbourne, Victoria, 3001, Australia

CONTENTS

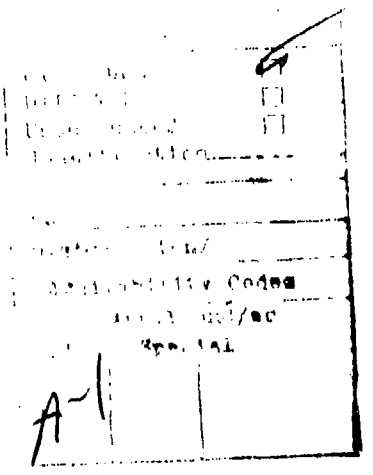

1. INTRODUCTION

Full-scale flight-by-flight fatigue tests on Mirage III aircraft structures have been carried out at the Aeronautical Research Laboratories (ARL) and the Eidgenössisches Flugzeugwerk (F+W), Switzerland. In the Australian wing test a catastrophic failure originated at the bottom of a blind hole in the lower flange of the main spar; while in the Swiss test the final failure also originated at the lower surface of the main spar but at a front flange bolt hole. The two failure locations are shown on Fig. 1, and are described in detail in References 1 and 2. In addition, fatigue cracks were identified at a number of other locations in the wing structure (Ref. 3).

An assessment of the test lives and crack growth rates determined by the fractographic examination of several of the fatigue fracture surfaces indicated that the fatigue performance of bolt and rivet holes along the front and rear lower flanges of the wing main spar would need to be improved if the the projected life-of-type of the aircraft was to be achieved. The three main areas of interest were:

(a) the interference-fitted 5 mm diameter fastener holes along the front flange of the spar;

(b) the inboard five bolt holes (8 mm and 10 mm diameter) along the rear flange, fitted with close-fit bolts; and

(c) the rear flange fastener holes (8 mm diameter) just outboard of those in area (*b*), also fitted with close-fit fasteners.

A detail of the relevant portion of the spar lower surface rear flange covering areas (*b*) and (*c*) is shown in Fig. 2. The investigation which forms the subject of this report relates to area (*c*) i.e. that portion of the spar (Figs 1 and 2) associated with the second gang-nut strip assembly. It was carried out mainly to provide preliminary information relating to the refurbishment techniques proposed for area (*b*) of the spar, some results for which have already been published in an interim report (Ref. 4). The two fatigue-life improvement techniques covered by the present investigation were cold-expansion of bolt and rivet holes and the installation of interference-fit steel bushes (both low-alloy and stainless steels) in bolt holes.

2. TEST SPECIMENS AND FATIGUE LOADING CONDITIONS

The main spar of the Mirage III is a large forging in aluminium alloy A-U4SG (equivalent to the American alloy 2014). Two pieces of 32 mm thick 2014-T651 aluminium alloy plate (ARL designation GJ) cut from a single larger piece were used for this investigation.* A total of 35 low-shear-load-transfer bolted joint fatigue specimens of the general type illustrated in Fig. 3 (which represented the 6th to 8th bolt holes along the rear flange and the associated through-the-flange rivets), and transverse tensile "control" specimens were manufactured from the positions in the plates shown in Fig. 4. The thickness of the fatigue test specimen (23 mm) corresponded to the nominal thickness of the spar flange at the 7th bolt hole. All fatigue specimens had their longitudinal axes parallel to the plate rolling direction. Compact tension fracture toughness specimens and "longitudinal" tensile specimens were taken from broken fatigue specimens at the positions shown in Fig. 5; and the results of the tests on these specimens, together with the chemical composition of the plate material, are given in Table 1.

For the basic fatigue "control" specimens the bolt holes were reamed to 8·013/8·035 mm diameter and the rivet holes drilled to 3·1 mm diameter. Assembly of the aluminium gang nut strip and packing shim to the body of the specimen was made using two 3 mm A-U4G rivets in the solution treated condition. After four days—to allow the rivets to precipitation-harden—the skin panel was fitted using the three 8 mm diameter close-fit high-tensile bolts which were tightened to a torque of 7·9 Nm (70 inch-lb) in the sequence holes 3, 1 and 4.

* The test material was supplied by Eidgenössisches Flugzeugwerk, Emmen, Switzerland.

The fatigue load spectrum adopted for this investigation (Fig. 6) was a simplified version (derived by Avions Marcel Dassault—AMD) of the Swiss Mirage full-scale flight-by-flight wing test spectrum. It was transformed into a 100-flight load sequence, the breakdown of this sequence into four different flight types (A^1, A, B and C) being given in Fig. 7. Cycles of $+6{\cdot}5$ g/$-1{\cdot}5$ g and $+7{\cdot}5$ g/$-2{\cdot}5$ g (a total of 39 cycles in 100 flights) were applied at a cyclic frequency of 1 Hz, whereas the remaining 1950 cycles per 100 flights were at 3 Hz. All fatigue tests were carried out in a servo-controlled electro-hydraulic fatigue machine (fitted with a 75,000 lbf MTS actuator and load cell), the 100-flight load sequence being achieved using an EMR Model 1641 programmable function generator controlled by a punched tape and in sine wave mode.

Fatigue loads were based on the assumption that $+7{\cdot}5$ g corresponded to a *gross area* stress* (not including the skin plate) of 205 MPa (29,680 psi), and that there was a linear stress/g relationship, i.e. the 1 g gross area stress was $27{\cdot}3$ MPa (3,960 psi). The value of 205 MPa was derived from the strain ($373{\cdot}29$ μstrain/g) measured during the 1979 strain survey of the left hand F+W Mirage test wing at gauge $1{\cdot}7$ T (Ref. 5). This gauge was located on the side of the rear flange of the spar adjacent to the 8th rear flange bolt hole. At $+7{\cdot}5$ g the testing machine load was nominally 260,000 N (58,200 lbf).

3. FATIGUE LIFE IMPROVEMENT TECHNIQUES

At the onset of the investigation it was considered that any method for extending the fatigue life of the relevant part of the Mirage wing spar would involve enlargement of the bolt holes for the purposes of:

(*a*) cleaning up for non-destructive inspection;

(*b*) accurate sizing for a subsequent operation; or

(*c*) complete removal of existing fatigue cracks.

The latter was regarded as an essential requirement and that, to provide additional confidence of crack removal, $0{\cdot}5$ mm depth of metal should be removed past the point at which a crack inspection indicated a "crack-free" condition, i.e. the minimum oversize diameter of a bolt hole would be 9 mm. Recognizing that sensitive rotating-probe eddy current equipment was being used for the inspection of bolt holes in the Mirage spar, the value of $0{\cdot}5$ mm in depth is consistent with the value of $0{\cdot}75$ mm shown by Butler (Ref. 6) and Galt (Ref. 7) to effectively remove fatigue damaged material beyond last visual crack indications.

Of the various refurbishment options available for the bolt holes those covered by this investigation were:

(i) cold-expansion ($2{\cdot}8\%$ or $3{\cdot}2\%$) by the Boeing split-sleeve process, and

(ii) interference-fitted ($0{\cdot}3\%$) steel bushes.

Consideration was also given to the adoption of a fatigue-life enhancement system, *ab initio*, as an alternative to reamed bolt holes for the basic design detail; and to the use of such systems in situations where, in service, fatigue crack removal could not be guaranteed.

3.1 Hole cold-expansion using the Boeing split-sleeve process

The Split-Sleeve Hole Cold-Expansion System was developed by the Boeing Company, Seattle, USA. It is described in detail in Reference 8 and summarised in Appendix 2 to this report. Radial plastic expansion of a hole by the Boeing or similar processes (such as the J. O. King, Ref. 9) results in the development of both radial and tangential (hoop) residual compressive stress fields in the material adjacent to the hole (Refs 9–16). The magnitude of the latter can equal the compressive yield strength of the material. An indication of the calculated and measured residual hoop stress distributions at the surface in 10 mm thick aluminium alloy (equivalent to 2024) after $4{\cdot}5\%$ hole cold expansion is given in Fig. 8 (Ref. 16). Although under

* The ratios of nett/gross areas at the bolt hole sections and rivet hole sections in the 'control' and refurbishment configurations are given in Appendix 1. For this material the modulus of elasticity was taken as 73×10^3 MPa ($10{\cdot}6\times10^6$ psi).

the action of external tensile loadings some relaxation in the magnitude of these residual stresses may occur, the compressive stresses effectively decrease the mean stress of the fatigue cycle near the hole and result in a retardation of the development of any fatigue cracks which may form at the surface of the hole by (for example) fretting (Refs 8, 13, 19-21). As a consequence, the fatigue life can be increased.

Furthermore, in order to introduce an effective compressive stress field, it is recommended that the distance from the hole edge to the adjacent edge of the component must exceed some specified minimum value. In Process Specification IWMF-2F76 issued by Industrial Wire and Metal Forming Inc. (the marketers of the Boeing system) the minimum edge margin—defined as the ratio of the distance from the hole centre line to the edge of the plate divided by the hole diameter—is specified as 2·0. For the basic specimen illustrated in Fig. 3 this ratio is 1·94.

For its first application in this investigation, i.e. as an alternative to a simple reamed hole, the starting hole size (7·633/7·684 mm diameter) was selected to enable an expansion of nominally 2·8% to be achieved, and a finished hole size (after reaming) of 8·013/8·035 mm diameter to suit the standard 8 mm diameter (7·985/8·000) close-fit bolts.

Secondly, it was considered as a potential life-extension technique to simulate a situation in which no guarantee could be given that pre-existing fatigue cracks would be removed during reaming prior to cold-expansion. Two series of tests were carried out, the first (basically a control series) in which the bolt holes in virgin specimens were cold-expanded (nominal cold-expansion 3·2%*) and reamed to 8·681/8·707 mm diameter to accept 8·6 mm diameter (8·653/8·669) oversize close-fit bolts; the second in which the cold-expansion and reaming procedures were carried out on three specimens after fatigue cracks of 8 to 12 mm indicated length had been developed along the bores of bolt holes. For this phase of the investigation non-destructive examination of the bolt holes (using a Förster "Defectomat F" rotating-probe eddy-current instrument) was conducted initially after 5,000 flights and at intervals of 2,000 or 3,000 flights thereafter. After the development of cracks of a suitable length the bolt holes were reamed to 8·420/8·425 mm diameter, re-examined for cracks, cold-expanded by 3·2% and reamed (as before) to accept 8·6 mm diameter bolts and finally again examined for cracks. Details of the cracks which were identified in these specimens are given in Table 2.

3.2 Interference-fitting of steel bushes

Lugs incorporating thin interference-fit bushes are relatively common in aircraft structures which require to be disassembled, but the bushing of small bolt holes in spars has been used only rarely—the Vickers 'Viscount' wing spar being one example. Compared with bushes fitted to lugs, those in bolt holes have a much greater bush length to hole diameter ratio.

Significant improvements in the fatigue performance of bushed compared with unbushed lugs have been reported (Ref. 22). These have been attributed, firstly, to a reduction in the relative movement between the bush and the lug hole (and hence a reduction in fretting) because of the radial pressure associated with the interference; and secondly, to the pre-stressing effect of the bush in the hole which effectively increases the tangential tensile mean stress at the boundary of the hole on the transverse diameter but reduces the local alternating stress range in the region of crack initiation under conditions of repeated external loading (Refs 23 and 24).

According to Gökgöl (Ref. 24) the optimum design for an interference-fit bush in a lug results in a bush thickness of 0·05 to 0·10 times the hole diameter; whereas Lambert and Brailey (Ref. 25) have stated that a bush must have a diameter ratio (external/internal) of greater than 1·33 to produce the same effective interference as a solid pin of the same external diameter and to avoid distortion of the bush which, in turn, could reduce the interference stresses. Taking an 11 mm external diameter bush as an example the wall thickness according to Gökgöl would be

* The slightly greater degree of expansion was necessitated by the tooling available at the time.

0·55 to 1·1 mm, and according to Lambert and Brailey 1·38 mm. Again, the first application considered for interference-fit bushed holes was that as an alternative to a simple reamed hole, but retaining the use of an 8 mm close-fit bolt. As information obtained from different sources in the aircraft industry suggested that a minimum wall thickness of 1·5 mm was desirable in such a situation for practical reasons, the smaller of the first two bushes had an outside diameter of 11 mm, and the larger 13 mm diameter. Furthermore, bushes of such diameter would, in a refurbishment situation, provide for the removal of cracks with indicated depths of 1 mm and 2 mm respectively; this being based on the premise that 0·5 mm depth of metal should be removed after the first crack inspection which indicated a "crack-free" condition. However, for increasing external diameters of bush there is a progressive increase in the nominal nett stress in the aluminium alloy at the bolt hole section and in the K_t value at the outer side of the hole (Ref. 26). For example, with the 13 mm bush specimen the nett area stress is about 12% greater than that in the "control" specimen.

Published data on the effects of interference-fit pins and bushes on the fatigue behaviour of aluminium alloy lugs (Refs 22, 27–31) indicate that significant improvements in fatigue life can be obtained with interferences of from 0·2% to 0·6% and that the extent of the improvement increases with the degree of interference. However, as the use of the higher degree of interference introduces practical problems in the insertion of long parallel bushes in holes of small diameter, a nominal interference of 0·3% was adopted for these tests to ensure that, within the range of accepted manufacturing tolerances for holes and bushes, an effective degree of interference of 0·25% to 0·35% could be achieved.

Details of the bushes are given in Figure 9. The bush material was either heat-treated SAE 4130 Cr-Mo Steel, or grades 304 or 316 chromium–nickel austenitic stainless steels—the stainless steels being used because of the potential requirement to have an eddy-current crack detection capability through the bushes. Tensile properties of these bush materials are given in the Appendix 3. The bushes were pressed into the specimens from the Datum Face using a small static testing machine, the sequence of bush insertion being holes 3, 1 and 4. A barium chromate paste was used as a lubricant and corrosion inhibitor during the insertion of all bushes; but, in addition, the stainless steel bushes were passivated in a nitric acid solution (Ref. 32) before insertion and, for these particular bushes, the corresponding holes in the specimens were given an Alodine 1200 treatment (Ref. 33) applied by brushing. Maximum bush insertion forces and (after specimen failure) the maximum bush removal forces are given in Table 3.

For the 0·25% to 0·35% interference-fitted bushes adopted in this particular specimen configuration the hoop stresses which are introduced into the aluminium alloy adjacent to the hole do not (theoretically) cause yielding of the material. Their magnitudes for various bush sizes (determined using the nomograms in Reference 34) are shown in Fig. 10. An experimental investigation of these stresses was undertaken by mounting strain gauges on the faces and side closest to the holes of specimen GJ2A15 (see Figs 11 and 12) and measuring the strain distribution with 13 mm diameter SAE 4130 steel bushes fully inserted and after their removal from the holes. The method of bush insertion is shown in Fig. 13 and details of this investigation given in Appendix 4.

The second series of tests involving interference-fit bushes considered the feasibility of fitting bushes to holes with existing fatigue cracks. Pre-cracking of the bolt holes in three specimens was carried out concurrently with those designated for subsequent cold-expansion, and details of the pre-cracking conditions are also given in Table 2. The bolt holes were subsequently reamed to 8·71 mm diameter and fitted with SAE 4130 steel bushes having an internal diameter of 6·35 mm (bush wall thickness of 1·18 mm), to accept the appropriate close-fit stepped bolts (Fig. 9) torqued to 7·9 Nm (70 inch-lb). For comparative purposes some tests were also made on virgin specimens fitted with 8·71 mm diameter bushes before fatigue testing.

After a failure, early in the testing program, from an as-reamed 3 mm rivet hole, all rivet holes in the first groups of cold-expanded and interference-fit bushed specimens were also cold-expanded and 5/32 inch (nominally 4 mm) diameter 2117 aluminium alloy rivets fitted to secure the gang-nut strips and shim before commencement of fatigue testing. For all bushed, cold-worked and pre-cracked specimens, reworking of the rivet holes in this way was done after the work on the bolt-holes (including bush insertion and refurbishing) had been completed. Details of the rivet hole cold-expansion techniques are also given in Appendix 2.

4. TEST RESULTS AND DISCUSSION

All fatigue test results together with details of the failure locations and fatigue cracking characteristics for each specimen are given in Table 4 and the fractures are shown diagrammatically in Fig. 14.* Photographs of representative fracture surfaces are illustrated in Fig. 15. The significance of the life to failure being associated predominantly with or close to flight 42 is that this flight contains the maximum load cycle (+7·5 g to −2·5 g) which occurs only once in each 100-flight sequence. Data relating to the average lives of the various types of specimens are summarised in Table 5.

A statistical analysis of the fatigue data indicated that, in every case, cold-expanding or bushing (Tables 4(*b*) to 4(*h*)) provides a significant increase in fatigue life compared with the average life of the 8 mm "control" specimens (Table 4(*a*)), irrespective of the increase in nominal nett area stress in the aluminium alloy at the bolt hole section because of the use of bushes of greater than 8 mm external diameter. The average lives of specimens with cold-expanded or bushed holes of 8 and 8·71 mm diameter (Tables 4(*b*) to 4(*d*)) are not significantly different, but are more than double that of the control group of specimens. Thus, both of these processes could provide valuable improvements in life compared with as-reamed holes of the same diameter in thick aluminium alloy sections.

A comparison of the data for the different bush materials (Table 4(*e*) and 4(*f*) and Table 4(*g*) and 4(*h*) respectively) shows that for both the 11 mm and 13 mm bushes there are no significant differences in the average lives resulting from the use of the low-alloy steel and stainless steel bushes. Furthermore, there are no significant differences in the average lives of specimens fitted with 11 and 13 mm diameter bushes. Although the analysis shows that the specimens fitted with 11 and 13 mm diameter low-alloy steel bushes have significantly greater average lives than that of specimens with 8·71 bushes, this result should be treated with caution because of the small sample size in the 8·71 mm case and the very low standard deviation of log. lives associated with this group. Nevertheless, providing any pre-existing cracks are completely removed by reaming, considerable extensions in fatigue life could be achieved by the use of quite large oversize interference-fit steel bushes. It should be noted that the cold-expanding of holes to these diameters in structural details of this type would be unacceptable because of the resulting small hole/edge distance.

However, when comparing the numerical values of the average lives in Tables 4(*a*) to 4(*h*) and in assessing the effects of cold-expanding, bushing, bush sizes and materials, the following observations should be noted and recognised. All of the 8 mm hole control specimens and all except one of the refurbished specimens failed from fatigue cracks which initiated along the bores of the holes or at a face/hole intersection, whereas the primary fatigue origins in about 70% of the other cold-expanded hole and bushed hole specimens were associated with fretting at either the plate or anchor-nut faces adjacent to a bolt hole but displaced along the length of the specimen by up to one radius from the minimum section, i.e. for these specimens the hole, as such, was no longer the most critical location—a general observation also made by Schütz (Ref. 35). Nevertheless, most of these specimens also exhibited varying degrees of secondary crack initiation along the bores of the bolt holes. This change of primary failure initiation associated with both cold-expanding and interference-fit bushing of the bolt holes would tend to mask the *specific* improvement in fatigue lives actually associated with these processes. As the six cold-expanded or bushed hole specimens which failed from primary crack initiation *along the bores* (i.e. GJ1S, GJ2A11, GJ2B15, GJ2B3, GJ2A9 and GJ2B10) had lives ranging from 39,042 to 57,580 flights with a log. average of 45,650 flights—2·37 times that of the 8 mm control group—the relative average lives indicated in Table 4 should therefore be regarded more as a lower limit to the improvement which could be expected if all failures had occurred primarily from crack initiation at the bolt holes.

---

* One specimen (GJ2A6) was tested in the unassembled condition, i.e. with all holes unfilled and without plates, etc., to investigate a crack detection system. It failed through hole (1) at a life of 13,542 flights. Specimen GJ2A15 was not fatigue tested but used for the measurement of strains around interference-fit bushes.

The information relating to residual fatigue cracks in refurbished specimens presented in Table 2 and the fracture surfaces illustrated in Figs 14(*j*) and 14(*k*) indicate that there were relatively large residual crack areas in three specimens (namely GJ2A4, GJ2A8 and GJ2A12), while those in specimens GJ2B1, GJ2B13 and GJ2A12 were relatively small. This is reflected both in the lives endured after refurbishment and the locations of the primary fatigue failures. In the case of the cold-expanded hole specimen GJ2B1, the primary failure was from fretting at the anchor-nut strip surface at a life of 48,242 flights after refurbishment—slightly greater than that of the average of the 8·71 mm cold-expanded control group (Table 4(*c*)); indicating that the cold-expansion had been effective in at least retarding crack growth from the residual fatigue crack. Cold-expanding of the bolt holes was less effective in the case of specimen GJ2A4, although the total life of 48,182 flights is significantly greater than the average of the 8 mm reamed-hole control group (19,250 flights). Similarly, whereas specimen GJ2B13 failed at a rivet hole its total life was significantly greater than that of this control group. These results lend support to those reported in Refs 15, 20 and 21 in showing that when small-size residual cracks are present the cold-expanding process could be used as a repair process to provide useful extensions in fatigue life.

The residual cracks in the refurbished 8·71 mm low-alloy steel bushed specimens were slightly larger than those in the refurbished cold-expanded hole specimens but, with the possible exception of specimen GJ2A12, the installation of the interference-fit bushes after refurbishment has not resulted in any significant improvement in the fatigue lives of these three specimens compared with those of the 8 mm reamed hole control group. This apparent lack of effectiveness of bushing to provide an extension in the fatigue lives of cracked specimens under these test conditions was not unexpected, when taking into consideration the findings of Petrak and Stewart (Ref. 20) that:

(*a*) cold-expansion or interference-fitting is more effective in retarding the growth of small rather than large cracks, and

(*b*) the amount of crack growth retardation is a function of the degree of cold-expansion or interference, with the greater retardation being associated with larger amounts of interference.

In this case it is likely that after the installation of the interference-fit bush the existing crack tip would be contained within a significant level of residual tensile hoop stress introduced by the bush; and although the cyclic stress range at the crack tip might be reduced accordingly, the stress intensity range has clearly not been reduced sufficiently to significantly retard the rate of crack propagation.

In only three of the 25 specimens in which the rivet holes were cold-expanded did the final fracture occur through the rivet holes, i.e. specimens GJ2A3, GJ2B10 and GJ2B13 at lives of 37,500, 45,442 and 33, 842 (total) flights respectively. The last of these was a refurbished specimen which contained a large residual crack at the No. 5 rivet hole as a result of prior fatigue loading. These lives should be compared with that of a specimen (GJ2B4) with non cold-expanded rivet holes which failed at No. 5 hole after 29,100 flights, and those of the other 22 bushed or cold-expanded hole specimens which had lives of between about 35,000 and 67,000 flights. Consequently, cold-expanding of the rivet holes was regarded as a satisfactory technique for reducing the incidence of premature failure at this location for specimens in which the bolt holes had been either cold-expanded or fitted with bushes.

Reference to Table 3 and Fig. 16 shows that the average force required to insert the bushes becomes greater with increasing diameter of bush (being 6940, 12770 and 16680 N for the 8·71, 11 and 13 mm diameter bushes respectively); and that, in all cases, the bush removal force for particular holes exceeded the bush insertion forces. The ratio of removal/insertion forces ranged from 1·17 to 4·19 with an average of 2·88. This general behaviour was to be expected because of the greater bush/hole surface contact area with increasing diameter of bush, the development of fretting between the bushes and the hole surface during fatigue cycling and the likelihood of little or no lubricant being retained at the bush/hole interface to reduce friction during bush removal. Although the overall correlation between bush insertion and removal forces is not good, the values provide some guidance as to the forces which might be required to remove bushes of these sizes after service in aircraft spars.

In addition to the non-destructive inspection of holes carried out prior to the refurbishment of specimens listed in Table 2, after fracture the "non-failure" bolt holes in all of the specimens were examined in the same way using the Förster "Defectomat F" rotating probe eddy-current instrument. Of the 68 holes examined in this way fatigue crack indications (Table 3) were found in a total of 18 unbushed (control or cold-expanded) holes—excluding specimen GJ2A6—and in eight bushed holes (after bush removal). These were mostly in the hole at the opposite end of the specimen to that at which the fracture had occurred, but in six of the 26 cases the middle hole (No. 3) gave crack indications.

Six of the eight holes in bushed specimens were subsequently opened up to expose the fatigue fracture surfaces. Details of the cracks in these specimens detected using the "Defectomat F" and those identified by fractography are given in Table 6, while the crack front shapes are illustrated in Fig. 17. For cracks exceeding about 4 mm in length (and about 1·5 mm in depth) the actual positions of the ends of the cracks were within about 1 mm of the positions estimated using the "Defectomat F", and in most cases the estimated crack length exceeded the actual length. However, in the case of cracks of less than about 2 mm in length and 1 mm in depth the quantitative identification of cracks in this situation by means of the "Defectomat F" is less certain. Cracks of less than 0·5 mm in depth were apparently not detected by the "Defectomat F". Nevertheless, these findings (albeit from limited data) do provide added confidence in the ability of the Defectomat to *detect* cracks of about 2 mm in length in the bores of holes, and to measure the lengths of such cracks with acceptable accuracy when this exceeds about 4 mm.

Of the 34 specimens tested, 23 finally fractured during the application of the "7·5 g" peak load cycle, and of the 16 instances where the final failing load was recorded it was between that corresponding to the "6·5 g" and "7·5 g" loads. In all other cases it was just less than the "6·5 g" load. However, the geometries and sizes of the fatigue cracks at failure relative to the cross-sectional dimensions of the specimens are not conducive to meaningful residual strength fracture analysis.

The results of strain measurements made during the insertion of bushes in specimen GJ2A15 with a nominal average interference of 0·28% are given in Appendix 4. After removal of the bushes the indicated hoop strains were virtually zero, confirming that the strains induced in the specimen by the bushes were elastic. By adapting the case of the hoop strains developed in a semi-infinite sheet containing a pressurized hole Jost (see Appendix 5) has calculated the hoop strain distribution introduced by a stainless steel bush of 0·28% interference in an aluminium alloy specimen along a line normal to the side of the specimen and passing through the centre of a hole. The predicted strain distributions compared with those calculated at the mid-point of the thickness of the specimen using the strain measurements are shown in Figs 18 and A5-2. It may be seen that there is an excellent agreement between the shapes of the actual and predicted hoop strain distributions, and quantitatively for the case (Cols. B, C of Table A4-1) of the specimen with slightly greater stiffness resulting from the installation of bushes in the adjoining holes. A comparison of the hoop stress at the edge of the hole calculated using the Jost analysis and the ESDU Data Sheet (Ref. 34) is shown in Fig. 10. This would suggest that the ESDU Data Sheets might over-estimate the numerical value of hoop stresses introduced by interference-fit bushes by some 20%.

5. CONCLUSIONS

1. In thick sections of aluminium alloy representing an aircraft spar flange the cold-expansion of bolt holes or the use of interference-fit steel bushes can at least double the fatigue life of a joint.
2. For slightly oversize holes there is no significant difference in the average lives for holes cold-expanded or those fitted with interference-fit steel bushes of the same external diameter.
3. No significant differences are apparent between the fatigue lives of specimens embodying low-alloy steel or stainless steel interference-fit bushes.

4. When small-sized residual fatigue cracks are present the hole cold-expansion process may be suitable for providing an extension in fatigue life.

5. The fitment of interference-fit steel bushes is not likely to be an effective method of extending fatigue lives in the presence of large-size residual fatigue cracks. However, if such cracks can be machined out, the incorporation of oversize interference-fit bushes could provide significant extensions in fatigue lives.

ACKNOWLEDGEMENTS

The authors wish to express their appreciation to members of the Structures Division staff of the Aeronautical Research Laboratories who carried out the tensile and fracture toughness tests and to staff of Materials Division for chemical analysis, alodining of holes and passivating of the stainless steel bushes. Special thanks are given to Messrs B. C. Bishop and N. T. Goldsmith for their help in the detection and measurement of cracks.

Thanks are also expressed to Messrs K. J. Kennedy and K. J. Coad of the Commonwealth Aircraft Corporation Ltd. for providing assistance with the cold-expansion and refurbishment of bolt holes, and for the progressive non-destructive inspections of refurbished specimens; and to Corporal S. Nicoll of the RAAF for photographing the fracture surfaces.

REFERENCES

1. Anderson, B. E., and Goldsmith, N. T : Prediction of crack propagation in Mirage wing fatigue test spar. *Dept. Defence Aero. Res. Labs Structure Note* 448/*Materials Note* 124, April 1978.

2. Goldsmith, N. T.: Fractographic examinations relevant to the F+W Mirage fatigue test. *Dept. Defence Aero. Res. Labs Materials Tech. Memo.* 371, August 1978.

3. Bruton, R. A.: Failures resulting from a fatigue test on a Mirage IIIO wing. *Dept. Defence Aero. Res. Labs Structures Tech. Memo.* 319, July 1980.

4. Mann, J. Y., Lupson, W. F., Machin, A. S., and Pell, R. A.: Interim report on investigation to improve the fatigue life of the Mirage IIIO wing spar. *Dept. Defence Aero. Res. Labs Structures Tech. Memo.* 334, August 1981.

5. Sparrow, J. G.: Tripartite Mirage programme report—December 1980. *Dept. Defence Aero. Res. Labs Structures Tech. Memo.* 326, February 1981.

6. Butler, J. P.: The rehabilitation of fatigue-weary structure. *Fatigue of aircraft structures.* ASTM STP No. 203, November 1957, pp. 29–46.

7. Galt, B. C.: An evaluation of fatigue life improvement processes. *Tech. Rep.* AFFDL-TR-68-138, October 1968.

8. Phillips, J. L.: Fatigue improvement by sleeve cold working. *SAE Paper* No. 73095, Oct. 1973.

9. Chandawanich, N., and Sharpe, W. N.: An experimental study of fatigue crack initiation and growth from cold-worked holes. *Engng Fract. Mech.*, Vol. 11, No. 4, 1979, pp. 609–620.

10. Impellizzeri, L. F., and Rich, D. L.: Spectrum fatigue crack growth in lugs. *Fatigue crack growth under spectrum loads.* ASTM STP 595, May 1976, pp. 320–338.

11. Chang, J. B.: Prediction of fatigue crack growth at cold-worked fastener holes. *J. Aircraft*, Vol. 14, No. 9, Sept. 1977, pp. 903–908.

12. Dietrich, G., and Potter, J. M.: Stress measurements on cold-worked fastener holes. *Advances in X-ray Analysis*, Vol. 20, 1977, pp. 321–328.

13. Schijve, J., Jacobs, F. A., and Meulman, A. E.: Flight simulation fatigue tests on lugs with holes expanded according to the split-sleeve cold work method. *Natl Lucht-Ruimtev. Lab. Rep.* NLR TR 78131U, 21 Sept. 1978.

14. Sha, G. T., Cowles, B. A., and Fowler, R. L.: Fatigue life of a cold-worked hole. *Emerging technologies in aerospace structures, design, structural dynamics and materials.* (Editor: J. R. Vinson). New York, ASME, 1980, pp. 125–140.

15. Cathey, W. H., and Grandt, A. F.: Fracture mechanics consideration of residual stress introduced by cold-working fastener holes. *Jnl Engng Mater. Technol.*, Vol. 102, Pt 2, Jan. 1980, pp. 85–91.

16. Lowak, H.: The influence of component size, type of loading sequence and load level on the fatigue improvement by cold working of holes. (In German). *Fraunhofer-Institut für Betriebsfestigkeit Ber.* No. FB-157, 1981.

17. Kollman, F. G., and Oenoez, E.: Die Eigennspannung in den Ringen eines elastisch—plastisch beanspruchten Querpressverbandes nach der Entlastung. *Forsch. Ing.-Wes.*, Vol. 45, No. 6, 1979, pp. 169–177.

18. Rich, D. L., and Impellizzeri, L. F.: Fatigue analysis of cold-worked and interference-fit fastener holes. *Cyclic stress-strain and plastic deformation aspects of fatigue crack growth.* ASTM STP 637, Dec. 1977, pp. 153–175.

19. Schijve, J., Brock, D., and Jacobs, F. A.: Fatigue tests on aluminium alloy lugs with special reference to fretting. *Nat! Lucht-Ruimtev. Lab. Rep.* TN-M.2103, March 1962.

20. Petrak, G. J., and Stewart, R. P.: Retardation of cracks emanating f fastener holes. *Engng Fract. Mech.*, Vol. 6, No. 2, Sept. 1974, pp. 275–282.

21. Toor, P. M.: Cracks emanating from pre-cracked cold-worked holes. *Engng Fract. Mech.*, Vol. 8, 1976, pp. 391–395.

22. Fisher, W. A. P., and Yeomans, H.: Further fatigue tests on loaded holes with interference-fit bushes. *Royal Aircr. Establ. Tech. Note* Structures 210, Nov. 1956.

23. Heywood, R. B.: *Designing against fatigue.* London, Chapman and Hall Ltd., 1962. (See pp. 225–227).

24. Gökgöl, O.: Estimation of endurance of light metal alloy lugs with interference-fit bushes. *Royal Aircr. Establ. Lib. Trans.* 1861, Aug. 1975.

25. Lambert, T. H., and Brailey, R. J.: The use of an interference-fit bush to improve the fatigue life of a pin-jointed connection. *Aeronaut. Q.*, Vol. 13, Pt 3, Aug. 1962, pp. 275–284.

26. Elastic stress concentration factors: geometric discontinuities in flat bars or strips of isotropic materials. *Engineering Sciences Data Item* No. 69020, Aug. 1969.

27. Morgan, F. G.: Static stress analysis and fatigue tests of interference-fit bushes. *Royal Aircr. Establ. Tech. Note* Structures 316, Aug. 1962.

28. Aubrey, E., and McLean, J. L.: The effect of clearance holes on the fatigue life of aluminium lugs. *Canadian Aeronaut. Space Jnl*, Vol. 10, No. 6, June 1964, pp. 181–183.

29. Buch, A. Fatigue properties of aircraft lugs with interference-fit. *Technion Israel TAE Rep.* No. 243, Feb. 1975.

30. Buch, A.: Fatigue and fretting of pin-lug joints with and without interference-fit. *Wear*, Vol. 43, No. 1, 1977, pp. 9–16.

31. Buch, A., and Berkovits, A.: Fatigue of 2024-T351 and 7075-T7351 Al-alloy lugs with and without interference-fit under manoeuvre spectrum loading. *Technion Israel TAE Rep.* No. 440, April 1981.

32. Commonwealth Aircraft Corporation Ltd.: Cleaning of corrosion-resistant and heat-resistant alloys. *CAC Process Specification* No. PR 1-4, Issue A, 5 May 1972, Clause 6.2.1.

33. Commonwealth Aircraft Corporation Ltd.: Application of chemical films to aluminium. *CAC Process Specification* No. PR2-12, Issue B, 26 Sept. 1979, Clause 6.3.

34. Stresses due to interference-fit pins and bushes in plates, strips or lugs. *Engineering Sciences Data Item* No. 71011, May 1971.

35. Schütz, W.: Improvement of fatigue strength by residual compressive stresses. *Atti del 2° convegno sulla fatica nelle strutture aerospaziali, Vol. 1.* Pisa, Vigo Cursi Editore, 27–29 Feb. 1980, pp. 2.1–2.13.

36. Jeffery, G. B.: Plane stress and plane strain in bipolar co-ordinates. *Phil. Trans. Royal Soc. Series A*, Vol. 221, 1921, pp. 265–293.

APPENDIX 1

Nett/Gross Area Stress Ratios for Various Hole Sizes
(Gross Area = 1265 mm²)

Nominal hole diameter (mm)	Nett/gross area ratio	Nominal edge distance (mm)	Stress conc. factor (K_t)*
Bolt holes 1, 3, 4			
8·02 (control)	0·854	11·49	3·20
8·71	0·842	11·15	3·25
11·0	0·800	10·00	3·40
13·0	0·764	9·00	3·60
Rivet holes 2, 5			
3·1 (control)	0·944	13·95	3·03
4·0 (5/32 inch)	0·927	13·50	3·05

* At side of holes when unfilled and non-bushed (Ref. 26).

APPENDIX 2

Hole Cold-Expansion Systems

(i) *Boeing split-sleeve system for bolt holes*

The Split Sleeve Hole Cold Expansion System was developed by the Boeing Company, Seattle, USA. Permanent radial expansion (plastic deformation) of a hole is achieved by pulling a hardened steel mandrel through a disposable pre-lubricated stainless steel split sleeve located inside the hole. The use of the thin steel sleeve prevents scoring damage on the hole surface, and elastic recovery of the sleeve allows it to be easily removed from the hole after withdrawal of the mandrel. However, a thin ridge produced by the split in the sleeve is left along the surface of the hole parallel to its axis and when accurate hole sizes are required—as for close-fitting bolts—it is necessary to remove the ridge and to finish the cold-worked hole by either a light reaming or broaching operation. For the high interference cold-working process the expansion—measured as the percentage difference in diameter between the starting hole size and the maximum diameter of the mandrel plus twice the sleeve thickness—is designed to be between 3·5% and 4%. For particular combinations of tooling, s r degrees of expansion can be achieved by adopting larger starting hole sizes—a practice w ch can be followed if stress corrosion is a potential problem.

In the present investigation a cold-expansion of about 3% was adopted. The nominal edge margin of 1·94 (defined as the distance from the hole centre line to the edge of the specimen divided by the hole diameter) is just less than the minimum value of 2·0 stipulated in Process Specification IWMF-2F76 issued by Industrial Wire and Metal Forming Inc., the marketers of the Boeing system. Details of the cold-expansion procedures used are as follows:

A. Hole finished size nominally 8·013/8·035 mm diameter

Starting hole diameter:	7·633/7·684 mm
Sleeve thickness:	0·203 mm
Mandrel diameter (maximum):	7·468 mm
Finished hole size:	8·013/8·035 mm diameter
Nominal cold expansion:	2·47 to 3·16%

B. Hole finished size nominally 8·681/8·707 mm diameter

Starting hole diameter:	8·420/8·425 mm
Sleeve thickness:	0·254 mm
Mandrel diameter (maximum):	8·186 mm
Finished hole size:	8·681/8·707
Nominal cold expansion:	3 19 to 3·25%

(ii) *Cold expansion of rivet holes*

Cold expansion of the rivet holes was achieved using a small tapered mandrel of the type described in Reference 4. No sleeves were employed but a lanoline grease used as a lubricant during the expansion operation. The holes were firstly reamed to 3·9 mm diameter and then cold-expanded by nominally 3·2% to finish at 3·97 mm. They were not reamed after cold expansion. Assembly of the gang-nut strip to the specimen was made using 4 mm diameter (nominal) rivets of 2117 aluminium alloy.

For this investigation the pre- and post-cold expansion reaming was done from face 'C' to face 'A' (see Fig. 3) while the cold expansion was from face 'A' to face 'C'. Hand finishing (by filing) of the two faces adjacent to the holes was carried out after the post-reaming operations to remove the surface deformation associated with the cold expansion and to ensure flat surfaces for the skin panel and packing shim to bear upon.

APPENDIX 3

Tensile Properties of Bush Materials

Material	0·1% PS MPa; psi	0·2% PS MPa; psi	UTS MPa; psi	Elongation (%)
Cr-Mo Steel SAE 4130† (MIL-S-6758)	879; 127,500	886; 128,500	987; 143,100	15·2
Stainless steel Type 316‡	443; 64,300	504; 73,100	738; 107,100	42·5
Stainless steel Type 304*	786; 114,200	874; 126,800	1017; 147,600	20·5

† 0·6875 inch diameter bar covered by CAC specification BA 4257.

‡ 0·625 inch diameter bar now covered by Specification QQ-S-763D: Type 316. Nominally 16% to 18% Cr, 10% to 14% Ni.

* 0·6875 inch diameter bar now covered by Specification QQ-S-763D: Type 304. Nominally 18% to 20% Cr, 8% to 12% Ni.

APPENDIX 4

Measurement of Strains Induced by Interference-Fit Bushes

Thirty-nine strain gauges (13 per hole) were attached to specimen GJ2A15 as indicated in Fig. 11, the exact positions of the centres of the gauges being given in Fig. 12. The bushes were made of SAE 4130 steel, and during their insertion the specimen was mounted in a horizontal position in a small screw-operated static testing machine as shown in Fig. 17. A 9 mm wide steel bar (with grooves cut in it to provide clearances for the bushes and strain gauge wiring) was used to support the specimen along its test section and transmit the force during the bush insertion. Light oil was used as a lubricant as the bushes were being inserted.

To determine the interferences, dimensional measurements were made on two diameters at right angles at several positions along both the bushes and the holes. Based on the combination of limits in each case the corresponding ranges of interference of the three holes were:

Hole 1: 0·25% to 0·29% (average 0·27%)

Hole 3: 0·23% to 0·27% (average 0·26%)

Hole 4: 0·27% to 0·31% (average 0·29%)

When the accuracies with which the holes could be measured are taken into account the differences in interference between holes are considered to be insignificant. The overall average was taken as 0·28%.

Two series of measurements of the hoop strains were made. In the first series the bushes were inserted successively in holes 3, 1 and 4, and the strains adjacent to each hole recorded as the bush was inserted and at maximum insertion both before and after the specimen was removed from the testing machine. Some time after all three bushes had been inserted they were pushed out in a similar way to which they were inserted (but in the reverse direction), but the strains present after removal were not recorded. The second series of tests involved holes 1 and 4 only. In this case the bush in hole 1 was re-inserted and, immediately after the strains were measured, it was removed and the strains again measured. This procedure was repeated for hole 4 with the corresponding bush.

The hoop strains adjacent to the holes with the bushes fully inserted but with the specimen removed from the machine are given in Table A4-1. The gauge positions are indicated in Fig. 17, where it should be noted that, for each hole, positions (*a*) and (*m*), (*b*) and (*l*), (*c*) and (*k*), (*d*) and (*j*), (*e*) and (*i*) are respectively equivalent for the datum Face C (from which direction the bush was inserted) and the opposite Face A.

Because of the equivalence in bush insertion conditions, i.e. only one bush in the specimen at a time, it was considered justified to pool the measured strains at hole 3 in the first series of test with those from holes 1 and 4 in the second series. Similarly the strains at holes 1 and 4 in the first series of tests were pooled. In this case the specimen was less flexible because of the presence of the interference-fit bush in hole 3. The average strains at the various gauge locations for the two groupings of holes are given in the second last and last columns respectively of Table A4-1.

In the second series of strain measurements the residual strains after bush removal were less than the limits of accuracy of strain measurement, which confirmed that the hoop stresses induced by the interference fitment of the bushes were elastic.

TABLE A4.1

Measured Hoop Strains with Bushes Fully Inserted

Gauge position	Hole 1			Hole 3		Hole 4			Average strains	
	Gauge No.	Strain		Gauge No.	Strain First series (A)	Gauge No.	Strain		Cols. A^1, A, B^1	Cols. B, C
		First series (B)	Second series (A^1)				First series (C)	Second series (B^1)		
(*a*)	39	560	520	34	510	29	420	290	440	490
(*b*)	38	980	910	33	830	28	880	540	760	930
(*c*)	37	740	750	32	740	27	1090	800	760	920
(*d*)	36	604	560	31	570	26	800	560	560	700
(*e*)	35	660	600	30	590	25	800	540	580	730
(*f*)	24	840	—	21	770	18	980	—	770	910
(*g*)	23	950	850	20	860	17	950	740	820	950
(*h*)	22	1090	910	19	970	16	940	1020	970	1020
(*i*)	15	960	760	10	850	5	770	700	770	870
(*j*)	14	1100	850	9	950	4	820	800	870	960
(*k*)	13	1990	1510	8	1500	3	1420	1360	1460	1710
(*l*)	12	1390	1080	7	1300	2	1770	990	1120	1580
(*m*)	11	730	560	6	630	1	880	500	560	810

Strain is given in microstrains. Accuracy of strain measurement is $\pm 20\,\mu$strain.

APPENDIX 5

Stress and Strain in a Semi-Infinite Sheet Containing a Pressurized Hole

by G. S. Jost

It has been shown in Appendix 4 of this Report that the interference levels used in the present study do not cause yielding. The situation is therefore wholly elastic, and the work of Jeffery (Ref. 36) on a pressurised hole in a semi-infinite sheet may be applied here to predict stress and strain distributions. Attention is confined to predictions along the y axis (Fig. A5-1), this being the line along which hoop strains were measured. Plane strain conditions are assumed throughout.

The hoop and radial stresses along the y axis are given by:

$$\sigma_\theta/p = M\{(\cosh\alpha \pm 1)[2\cosh\alpha_1 \sinh\alpha \mp 4\sinh(2\alpha-\alpha_1)] \pm 2\sinh\alpha\cosh(2\alpha-\alpha_1)+\sinh\alpha_1+\sinh(2\alpha-\alpha_1)\} \quad \text{(A1)}$$

and

$$\sigma_r/p = -M\{(\cosh\alpha \pm 1)2\cosh\alpha_1 \sinh\alpha \mp 2\sinh\alpha\cosh(2\alpha-\alpha_1)-\sinh\alpha_1-\sinh(2\alpha-\alpha_1)\} \quad \text{(A2)}$$

where the upper signs are for that section of the sheet between the free edge and the nearest hole boundary, the lower signs for the region from the opposite side of the hole boundary to infinity.

Referring to Fig. A5-1, p is the applied pressure,

$$M = 0{\cdot}5\,\mathrm{csch}^3\alpha_1$$

$$\alpha_1 = \operatorname{arcosh} e/R$$

$$\alpha = \operatorname{arcosh}\left|\frac{y^2+a^2}{y^2-a^2}\right|$$

and

$$a^2 = e^2-R^2$$

Thus, for a given geometry (i.e. e and R), the hoop and radial stresses at points y along the ordinate may be calculated from (A1) and (A2) in terms of an internal pressure p applied to the hole. Between the sheet edge and the hole, $0 \leqslant y \leqslant e-R$ and from the hole to infinity $e+R \leqslant y \leqslant \infty$.

Under plane strain conditions, the hoop strain ϵ_θ is given by:

$$\epsilon_\theta = \frac{p}{E}\left(1-\nu^2\right)\left(\frac{\sigma_\theta}{p}-\frac{\nu}{1-\nu}\frac{\sigma_r}{p}\right) \quad \text{(A3)}$$

where the stress terms, given by (A1) and (A2), are functions only of geometry, ν is Poisson's ratio and E is Young's modulus.

For holes containing interference-fit pins or bushes, it is appropriate to work in terms of the diametral interference, δ, rather than the resulting interface pressure, p. In axisymmetric situations (e.g. a hole in an infinite plate or a thick-walled cylinder) exact relations between p and δ may be readily found. For non-axisymmetric cases, however, interference-fit pins or bushes do not result in a uniform interface pressure around the hole and so the uniform pressure theory cannot be directly applicable. It can, however, be effectively used in an approximate way by calculating the *average* radial expansion of the hole under the uniform pressure and using this to relate p to δ.

The average (plane strain) radial displacement of a pressurised hole in a semi-infinite sheet is given by:

$$u_s = pR\,\frac{1+\nu_s}{E_s}\,[\nu_s+(1-\nu_s)(2\ coth\ \alpha_1-1)] \tag{A4}$$

where the subscript s refers to the sheet.

For a bush, of inner and outer radii r and R respectively, under external pressure p, the (plane strain) radial displacement of the outer boundary is:

$$u_b = -pR\,\frac{1+\nu_b}{E_b}\left[\frac{R^2(1-2\nu_b)+r^2}{R^2-r^2}\right] \tag{A5}$$

where the subscript b refers to the bush.

The sum of the magnitudes of these two displacements must equal the radial interference, $\delta/2$, so that

$$\frac{\delta}{2} = |\,u_s\,| + |\,u_b\,|$$

or in terms of a non-dimensional $\lambda = \delta/2R$,

$$\lambda = p\left\{\frac{1+\nu_s}{E_s}\left[\nu_s+(1-\nu_s)(2\ coth\ \alpha_1-1)\right]+\frac{1+\nu_b}{E_b}\left[\frac{R^2(1-2\nu_b)+r^2}{R^2-r^2}\right]\right\} \tag{A6}$$

Equation (A6) provides an estimate of p for the semi-infinite case when interference, geometry and the elastic properties of both bush and sheet are known. The corresponding formulation for a bush in a hole in an infinite sheet is

$$\lambda = p\left\{\frac{1+\nu_s}{E_s}+\frac{1+\nu_b}{E_b}\left[\frac{R^2(1-2\nu_b)+r^2}{R^2-r^2}\right]\right\} \tag{A7}$$

Equation (A6) has been used to provide an estimate of p for the present case where

$$\lambda = 0{\cdot}28/100$$

$$E_b = 207\times10^3\ \text{MPa (4130 steel bush)}$$

$$E_s = 73\times10^3\ \text{MPa (aluminium alloy plate)}$$

$$\nu_b = \nu_s = 1/3$$

$$r = 4{\cdot}0\ \text{mm}$$

$$R = 6{\cdot}5\ \text{mm}$$

$$e = 15{\cdot}55\ \text{mm}$$

and

$$\alpha_1 = arcosh\ e/R = 1{\cdot}515$$

as

$$p = 100\ \text{MPa}.$$

The corresponding infinite sheet value is, from (A7), $p = 109$ MPa. Thus the boundary near the hole in the semi-infinite sheet has, according to this estimate, resulted in a reduction in average pressure between the bush and the sheet of about 9% in comparison with the infinite sheet case. (Plane stress assumptions for both bush and sheet lower the above estimates of p by about 7%). The above value of $p = 100$ MPa has been used, along with the above parameter values relating to the sheet under study to calculate the stress and hoop strain distributions along a line normal to the free edge of the sheet passing through the centre of the hole. These are tabulated in Table A5-1, the hoop strain distribution being shown in Fig. A5-2. On this diagram the averaged measured strain data values* are also shown. Agreement between observation and prediction is seen to range from good to excellent.

* Refer to columns headed Average Strains in Table A4-1. Values at corresponding radii on upper and lower faces have been averaged.

TABLE A5.1

Stresses and Strains for Semi-Infinite Sheet

$(2{\cdot}385-y/R)$*	σ_θ/p	σ_r/p	ϵ_θ**	Position on Fig. A5-1
2·385	0·854	0	1035	A
2·2	0·726	−0·017	891	
2·0	0·649	−0·067	828	
1·8	0·622	−0·147	843	
1·6	0·639	−0·262	934	
1·4	0·704	−0·426	1112	
1·2	0·824	−0·661	1400	
1·0	1·0	−1·0	1819	B
−1·0	1·0	−1·0	1819	C
−1·5	0·470	−0·424	827	
−2·0	0·271	−0·214	458	
−3·0	0·122	−0·067	188	
−4·0	0·067	−0·021	94	

* Abscissa plotting position on Fig. A5-2.

** Microstrain.

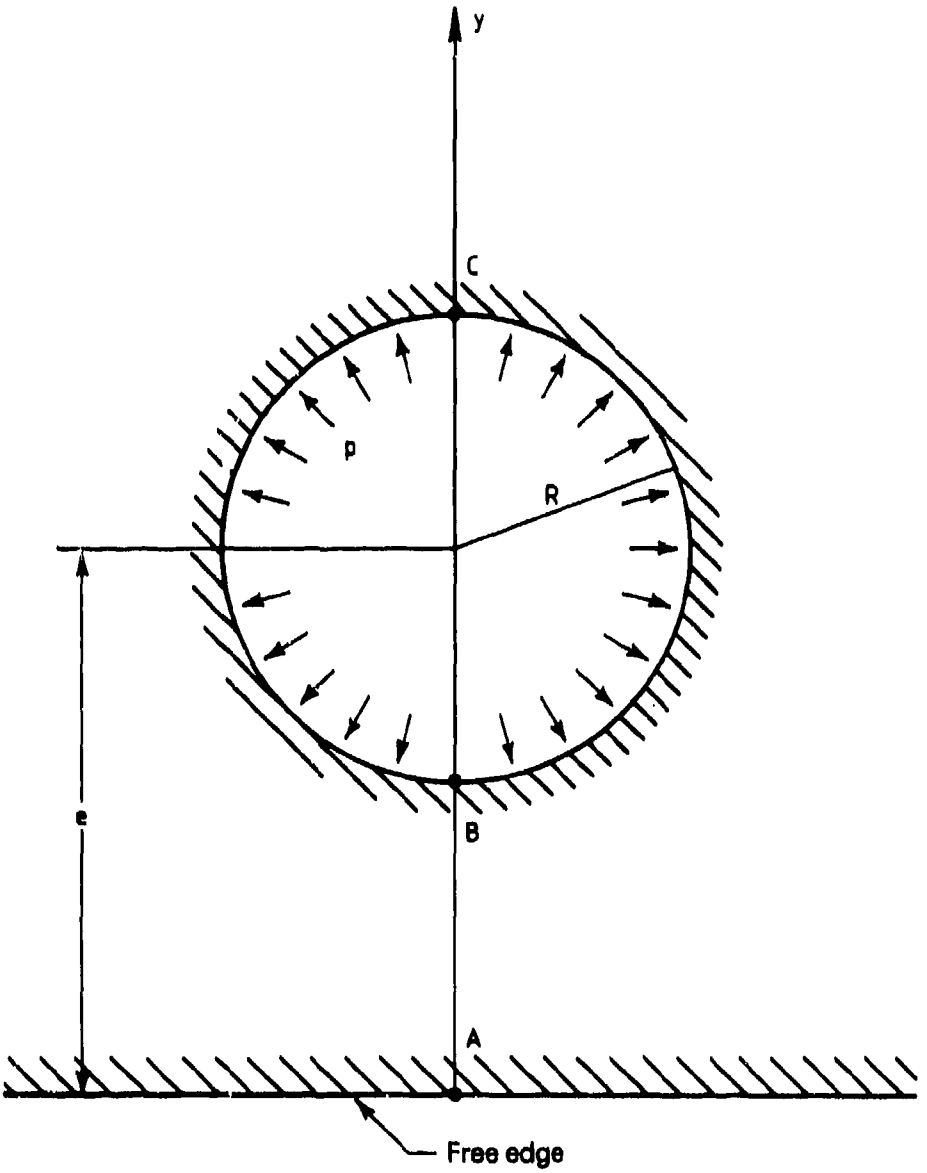

FIG A5-1 NOTATION FOR SEMI-INFINITE SHEET CONTAINING A PRESSURISED HOLE

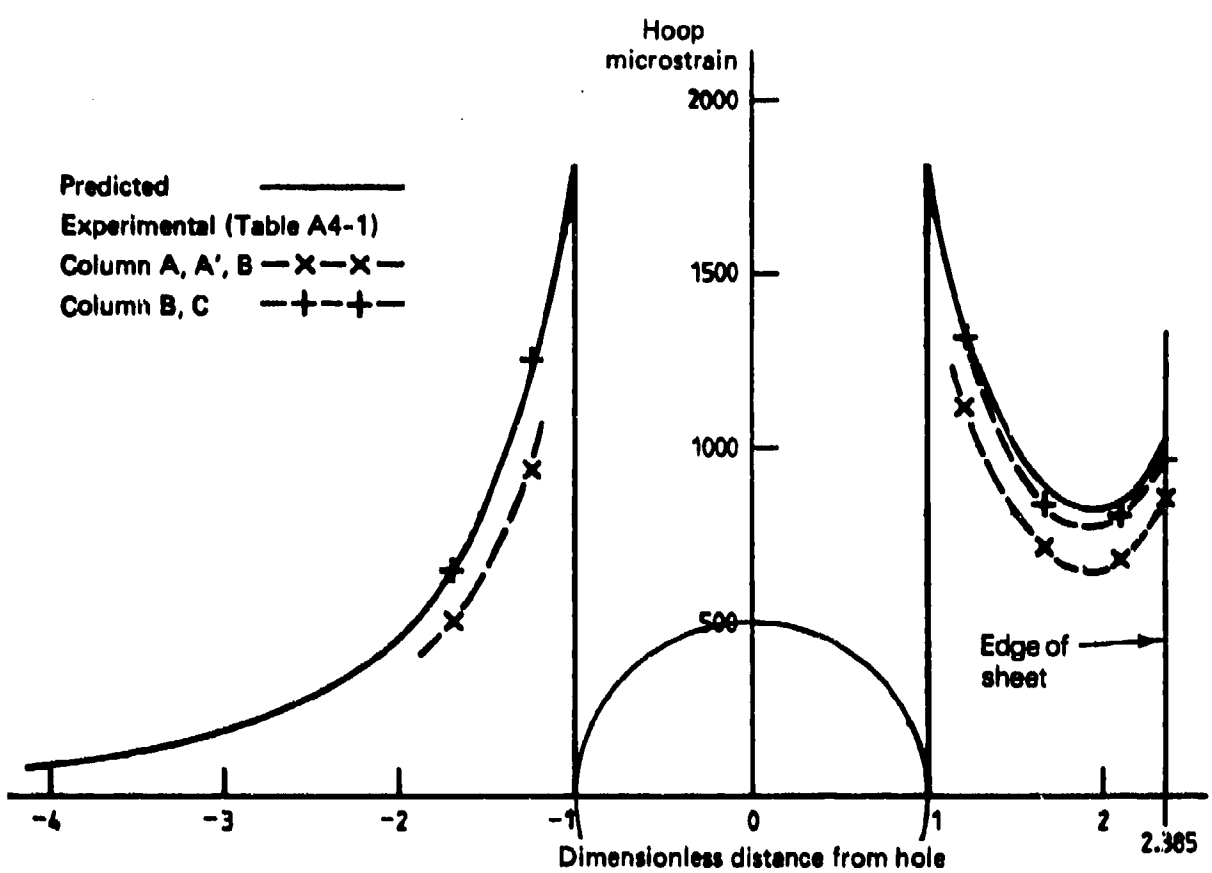

FIG. A5-2 PREDICTED PLANE STRAIN HOOP STRAIN DISTRIBUTION ALONG y AXIS (FIG A5-1) AND EXPERIMENTAL DATA POINTS (Appendix 4)

TABLE 1

Properties of Test Material

(a) Chemical composition

Element	*Specification (%)	Average of six samples (%)
Cu	3·9–5·0	4·48
Si	0·5–1·2	0·86
Mn	0·4–1·2	0·91
Mg	0·2–0·8	0·61
Fe	1·0 max.	0·45
Cr	0·1 max.	0·04
Zn	0·25 max.	0·12

(b) Static tensile properties

	*Specification (transverse)	Transverse (average of 4 tests)	Longitudinal (average of 6 tests)
0·1% PS, MPa (psi)	— (—)	458; sd 2† (66,500; sd 260)	470; sd 3 (68,200; sd 450)
0·2% PS, MPa (psi)	(59,000)	466; sd 1 (67,600; sd 170)	475; sd 3 (68,900; sd 410)
UTS, MPa (psi)	(67,000)	506; sd 3 (73,400; sd 460)	509; sd 3 (73,900; sd 390)
Elongation $(5{\cdot}65\sqrt{A})$, (%)	4	8·5 sd 0·9	9·3 sd 1·2
0·1% PS/UTS	—	0·91	0·92

(c) Fracture toughness

Specimen number	K_{IC}	
	MPa $m^{\frac{1}{2}}$	ksi $in^{\frac{1}{2}}$
GJ1B2	24·2	22·0
GJ1B3	24·6	22·4
GJ1B4	24·1	21·9
GJ1J3	25·7	23·4
GJ1J4	26·6	24·2
Average	25·0	22·8
sd	1·1	1·0

* Specification QQ-A-255a, 21 Feb. 1956, T651 condition, i.e. solution heat treated, stress relieved by stretching to produce a permanent set of 1·5 to 3%, and artificially aged.
† sd = standard deviation.

TABLE 2
Pre-cracking Details of Refurbished Specimens

Spec. No. GJ	Total life prior to refurbishment (flights)	Hole condition	Hole No.		
			Bolt hole 1	Bolt hole 4	Rivet hole 5
		(a) Bolt Holes Cold Expanded			
2B1	9,000	Reamed 8 mm	*Inner side:* 4·5 mm down, 10 mm long, 60%	NCD	—
		Reamed 8·4 mm	6 mm down, 8 mm long, 20%	NCD	—
		Cold-expanded and reamed 8·71 mm	6 mm down, 7 mm long, 10%	NCD	—
		Drilled 3·1 mm	—	—	NCD
		Reamed 3·9 mm	—	—	NCD
		Cold-expanded 4 mm	—	—	NCD
2A4	20,042	Reamed 8 mm	*Outer side:* 2·5 mm down, 12 mm long, 60%	*Outer side:* 2·5 mm down, 4 mm long, 10%	—
		Reamed 8·4 mm	3 mm down, 10 mm long, 25%	NCD	—
		Cold-expanded and reamed 8·71 mm	3 mm down, 9 mm long, 15%	NCD	—
		Drilled 3·1 mm	—	—	NCD
		Reamed 3·9 mm	—	—	NCD
		Cold-expanded 4 mm	—	—	NCD

TABLE 2 (continued)

Spec. No. GJ	Total life prior to refurbishment (flights)	Hole condition	Hole No.		
			Bolt hole 1	Bolt hole 4	Rivet hole 5
2B13	21,000	Reamed 8 mm	*Outer side:* (i) 8 mm down; 5 mm long, 20% (ii) 3–3 mm down, 5% *Inner side:* 0–5 mm down, 50%	*Outer side:* 1 mm down, 4 mm long, 20% *Inner side:* 3 mm down, 11 mm long, 40%	—
		Reamed 8·4 mm	*Outer side:* (i) 7 mm down, 3 mm long, 20%. (ii) NCD. *Inner side:* 0–5 mm down, 60%	*Outer side:* 0–4 mm down, 15% *Inner side:* 5 mm down, 5 mm long, 10%	—
		Cold-expanded and reamed 8·71 mm	*Outer side:* 7 mm down, 3 mm long, 10% *Inner side:* 0–3 mm down, 50%	*Outer side:* 0–3·5 mm down, 10% *Inner side:* 4·5 mm down, 6 mm long, 10%	—
		Drilled 3·1 mm	—	—	0–5 mm down, 40%
		Reamed 3·9 mm	—	—	0–5 mm down, 30%
		Cold-expanded 4 mm	—	—	0–5 mm down, 30%
		Countersunk 4 mm	—	—	0–5·5 mm down, 30%

TABLE 2 (continued)

Spec. No. GJ	Total life prior to refurbishment (flights)	Hole condition	Hole No.		
			Bolt hole 1	Bolt hole 4	Rivet hole 5
		(b) Bolt Holes Bushed			
2A8	15,000	Reamed 8 mm	*Outer side:* 0–2 mm down, 30% *Inner side:* 5 mm down, very small, 5%	*Outer side:* 0–10 mm down, 50%	—
		Reamed 8·4 mm	*Outer side:* 0–1·5 mm down, 10% *Inner side:* NCD	*Outer side:* (i) 0–2·5 mm down, 15% (ii) 3 mm down, 5 mm long, 50%	—
		Reamed 8·71 mm	*Outer side:* 0–2 mm down, 10%	*Outer side:* (i) 0–2·5 mm down, 10% (ii) 3 mm down, 4 mm long, 35%	—
		Drilled 3·1 mm	—	—	NCD
		Reamed 3·9 mm	—	—	NCD
		Cold-expanded 4 mm	—	—	NCD
Note: Bolt hole No. 4. After bushing, visual crack indication from outer side of bush to edge of specimen at plate surface.					
2B7	19,000	Reamed 8 mm	*Outer side:* (i) 10 mm down, 9 mm long, 25% (ii) 0–5 mm down, 40% *Inner side:* 2 mm down, 2–5 mm long	*Outer side:* 0–3·5 mm down, 20%	—
		Reamed 8·4 mm	*Outer side:* (i) 10 mm down, 8 mm long, 25% (ii) 0–4 mm down, 50% *Inner side:* NCD	*Outer side:* 0–2·5 mm down, 10%	—

TABLE 2 (continued)

Spec. No. GJ	Total life prior to refurbishment (flights)	Hole condition	Hole No.		
			Bolt hole 1	Bolt hole 4	Rivet hole 5
2B7 (cont.)		Reamed 8·71 mm	*Outer side:* (i) 10 mm down, 7·5 mm long, 15% (ii) 0–4 mm down, 40%	NCD	—
		Drilled 3·1 mm	—	—	NCD
		Reamed 3·9 mm	—	—	NCD
		Cold-expanded 4 mm	—	—	NCD
Note: Bolt hole No. 1. After bushing, visual crack indication 2 mm from outer side of bush running toward edge of specimen at plate surface.					
2A12	23,000	Reamed 8 mm	*Outer side:* (i) 8·5 mm down, 8·5 mm long, 30% (ii) 0–2 mm down, 35%	*Inner side:* 9 mm down, 8 mm long, 10%	—
		Reamed 8·4 mm	*Outer side:* (i) 14 mm down, 3·5 mm long, 15% (ii) 0–2 mm down, 60%	NCD	—
		Reamed 8·71 mm	*Outer side:* (i) 14 mm down, 3·5 mm long, 10% (ii) 0–2 mm long, 30%	NCD	—
		Drilled 3·1 mm	—	—	NCD
		Reamed 3·9 mm	—	—	NCD
		Cold-expanded 4 mm	—	—	NCD

Notes: NCD = No Cracks Detected.
Distance to end of crack measured from 'plate' surface.
Percentages are crack signal height as proportion of screen height, and are a qualitative indication of crack depth.
No cracks were detected in any specimen at Bolt hole No. 3 and Rivet hole No. 2.
— = not relevant.

TABLE 3

Bush Insertion and Removal Forces

Spec. No. GJ	Hole No.	Bush		Maximum forces (N)		Ratio removal / insertion	Cracks after failure
		Material	External diam. (mm)	Insertion	Removal		
2A3	1	LAS	8·71	4670	19570	4·19	ND
	3	LAS	8·71	8450	23130	2·74	ND
	4	LAS	8·71	6670	25800	3·87	NM
2A11	1	LAS	8·71	6230	24910	4·00	ND
	3	LAS	8·71	9340	33810	3·62	ND
	4	LAS	8·71	7560	failure	—	—
2B15	1	LAS	8·71	5340	18240	3·42	*
	3	LAS	8·71	7120	24910	3·50	ND
	4	LAS	8·71	8010	failure	—	—
2B4	1	LAS	11	15350	32920	2·14	*
	3	LAS	11	16900	34700	2·05	ND
	4	LAS	11	16010	18680	1·17	ND
2B3	1	LAS	11	10900	32030	2·94	*
	3	LAS	11	8010	18680	2·33	*
	4	LAS	11	11570	failure	—	—
2B12	1	LAS	11	14460	33360	2·31	*
	3	LAS	11	16010	33360	2·08	ND
	4	LAS	11	13790	failure	—	—
2A1	1	316 SS	11	9790	failure	—	—
	3	316 SS	11	11120	35590	3·20	ND
	4	316 SS	11	10680	35590	3·33	NM
2A9	1	316 SS	11	13340	failure	—	—
	3	316 SS	11	12460	34700	2·79	ND
	4	316 SS	11	11120	35590	3·20	*
2A5	1	LAS	13	17790	47150	2·65	*
	3	LAS	13	20020	41370	2·07	ND
	4	LAS	13	16680	failure	—	—

TABLE 3 (continued)

Spec. No. GJ	Hole No.	Bush		Maximum forces (N)		Ratio removal / insertion	Cracks after failure
		Material	External diam. (mm)	Insertion	Removal		
2B2	1	LAS	13	15570	48930	3·14	ND
	3	LAS	13	11300	47600	4·21	ND
	4	LAS	13	11300	failure	—	—
2A7	1	316 SS	13	12230	failure	—	—
	3	316 SS	13	12680	46710	3·68	ND
	4	316 SS	13	11790	41810	3·55	ND
2B10	1	316 SS	13	15120	53380	3·53	ND
	3	316 SS	13	26690	47150	1·77	ND
	4	316 SS	13	13340	21350	1·60	ND
2B14	1	316 SS	13	21130	failure	—	—
	3	304 SS	13	22240	48040	2·16	ND
	4	316 SS	13	22240	54710	2·46	ND
2A13	1	304 SS	13	18900	59160	3·13	ND
	3	304 SS	13	14460	invalid	—	*
	4	304 SS	13	13340	failure	—	—
2B8	1	304 SS	13	21130	failure	—	—
	3	304 SS	13	18900	44480	2·35	ND
	4	304 SS	13	13340	46260	3·47	ND
2A8	1	LAS	8·71	7340	24020	3·27	ND
	3	LAS	8·71	6670	17350	2·60	ND
	4	LAS	8·71	6890	failure	—	—
2B7	1	LAS	8·71	7560	failure	—	—
	3	LAS	8·71	7120	16900	2·38	ND
	4	LAS	8·71	6670	16460	2·47	ND
2A12	1	LAS	8·71	6230	failure	—	—
	3	LAS	8·71	5340	15120	2·83	ND
	4	LAS	8·71	7560	24020	3·18	ND

Notes: LAS = low-alloy steel; SS = stainless steel
ND = no cracks detected using rotating probe eddy current system
NM = cracks too small to be measured
* = see Table 6 and Fig. 17.

TABLE 4

Fatigue Lives and Fracture Details

Spec. No. GJ	Life to failure (flights)	Failing load (kN)	Failure details	
			Hole No.	Cracking
		(a) CONTROL (8 mm bolt hole)		
2A2	13,842	252·2	1	Origins both sides of hole 3 to 5 mm from 'plate surface'
1R	14,025	NR	1	Main origins outer side of hole about 3 mm and 8 mm from 'plate' surface; small cracks inner side
2B5	18,190	220·2	1	Main origin outer side of hole about 3 mm from 'plate' surface. Multiple cracks along inner side of hole
2A14	26,042	244·2	1	Main origin inner side of hole at 'A/N strip' surface. Multiple cracks along outer side of hole
2B11	28,742	233·5	4	Main origin inner side of hole about 2 mm from 'A/N strip' surface. Secondary crack outer side near 'plate' surface and multiple cracks along outer side of hole
Log. average life (flights) = 19,250 s.d. of log. life = 0·148				
		(b) BOLT HOLES BOEING COLD-EXPANDED 2·8% (8 mm diam.)		
1T*	33,742	243·3	4	Main origin at 'A/N strip' surface between outer side of hole and edge of specimen. Minor origins inner side of hole
1N‡	42,442	246·0	4	Ditto
1P*	48,642	256·2	4	Main origin at 'plate' surface about 6 mm from inner side of hole. Small cracks other corners
1S‡	50,817	NR	1	Major origin outer side of hole about 1·5 mm from 'plate' surface. Minor origins along both sides of hole
Log. average life (flights) = 43,376 s.d. of log. life = 0·080				
		(c) BOLT HOLES BOEING COLD-EXPANDED 3·2% (8·71 mm diam.)		
2B9‡	35,342	251·3	4	Main origin at 'plate' surface between outer side of hole and edge of specimen. Multiple origins along inner side of hole
2A10‡	41,342	249·5	4	Ditto, with multiple origins along both sides of hole
2B6‡	42,442	NR	4	Main origin at 'A/N strip' surface between outer side of hole and edge of specimen. Multiple origins along hole inner side
Log. average life (flights) = 39,582 s.d. of log. life = 0·043				

TABLE 4 (continued)

Spec. No. GJ	Life to failure (flights)	Failing load (kN)	Failure details	
			Hole No.	Cracking
(d) BOLT HOLES LOW-ALLOY STEEL BUSH 8·71 mm diam. (0·3 % Interference)				
2A3‡	37,500	NR	5	Origins both sides of rivet hole just in from 'A/N strip' surface
2A11‡	39,042	240·2	4	Two origins along outer side of hole 3 mm and 10 mm from 'plate' surface. Secondary crack 'plate' surface near inner side of hole
2B15‡	39,142	254·0	4	Major origin inner side of hole about 3 mm from 'plate' surface
Log. average life (flights) — 2A11 and 2B15 = 39,092				
s.d. of log. life = 0·001				
(e) BOLT HOLES LOW-ALLOY STEEL BUSH 11 mm diam. (0·3% Interference)				
2B4*	29,100	NR	5	Origins both sides of rivet hole just in from 'A/N strip' surface
2B3‡	44,542	244·2	4	Main origins along outer side of hole about 1·5 mm and 10 mm from 'plate' surface
2B12‡	49,942	250·0	4	Main origin at 'plate' surface about 7 mm from outer side of hole. Multiple cracking along inner side of hole.
Log. average life (flights) — 2B3 and 2B12 = 47,165				
s.d. of log. life = 0·035				
(f) BOLT HOLES 316 STAINLESS STEEL BUSH 11 mm diam. (0·3% Interference)				
2A1‡	55,842	224·2	1	Main origin 'A/N strip' surface about 3 mm from inner side of hole
2A9‡	57,580	220·6	1	Main origin outer side of hole at 'plate' surface. Multiple cracking along inner side of hole
Log. average life (flights) = 56,704				
s.d. of log. life = 0·009				
(g) BOLT HOLES LOW-ALLOY STEEL BUSH 13 mm diam. (0·3% Interference)				
2A5‡	40,778	208·2	4	Main origin 'plate' surface about 3 mm from outer side of hole. Secondary cracking along inner side of hole
2B2‡	63,642	240·2	4	Main origin 'A/N strip' surface about 2 mm from outer side of hole
Log. average life (flights) = 50,943				
s.d. of log. life = 0·137				

TABLE 4 (Continued)

Spec. No. GJ	Life to failure (flights)	Failing load (kN)	Failure details	
			Hole No.	Cracking
(h) BOLT HOLES STAINLESS STEEL BUSH 13 mm diam. (0·3% Interference)				
2A7‡ (316)	38,200	NR	1	Main origin 'A/N strip' surface close to outer side of hole. Secondary cracking along inner side of hole
2B10‡ (316)	45,442	256·2	5	Main origin inner side of hole just in from 'A/N strip' surface. Secondary crack outer side of hole near 'A/N strip surface'
2B14‡ (316)	46,542	244·0	1	Main origin 'plate' surface about 4 mm from outer side of hole. Multiple origins along inner side of hole
Log. average life (flights)—2A7 and 2B14 = 42,165				
s.d. of log. life = 0·061				
2A13‡ (304)	57,100	NR	4	Origins 'plate' surface about 2 mm from outer side of hole and 4 mm from inner side of hole
2B8‡ (304)	67,142	255·3	1	Origins 'plate' surface about 5 mm from inner side of hole, and 'A/N strip' surface about 2 mm from outer side of hole
Log. average life (flights) = 61,918				
s.d. of log. life = 0·050				
Log. average life (flights) 2A7, 2B14, 2A13, 2B8 = 51,096				
s.d. of log. life = 0·106				
(i) REFURBISHED, BOLT HOLES COLD-EXPANDED 3·2% (8·71 mm diam.)				
2B1	†(9,000)+48,242 = 57,242	235·8	1	Main origin 'A/N strip' surface about 3 mm from outer side of hole. Multiple crack initiation along both sides of hole
2A4	†(20,042)+28,140 = 48,182	NR	1	Main origin along outer side of hole about 5 mm from 'plate' surface (from pre-existing crack). Minor cracking along inner side of hole
2B13	†(21,000)+12,842 = 33,842	NR	5	Main origin outer side of hole at countersink of rivet from pre-existing crack. Multiple origins at other four corners of hole
Log. average *total* life (flights) 2B1 and 2A4 = 52,517				
s.d. of log. life = 0·053				

TABLE 4 (Continued)

Spec. No. GJ	Life to failure (flights)	Failing load (kN)	Failure details	
			Hole No.	Cracking
(j) REFURBISHED, BOLT HOLES LOW-ALLOY STEEL BUSH 8·71 mm diam.				
2A8	†(15,000)+8,842 = 23,842	227·7	4	Main origin from pre-existing crack about 5 mm along hole outer side from 'plate' surface. Multiple origins along inner side of hole
2B7	†(19,000)+3,842 = 22,842	249·1	1	Main origins outer side of hole about 2 mm along hole from 'plate' surface (pre-existing crack) and about 13 mm from 'plate' surface
2A12	†(23,000)+12,130 = 35,130	NR	1	Main origins outer side of hole about 1 mm and 15 mm along hole from 'plate' surface. Multiple origins along inner side of hole.
Log. average *total* life (flights) = 26,746 s.d. of log. life = 0·103				

* rivet holes reamed, 5/32 inch 2117 rivets.
‡ rivet holes cold-expanded, 5/32 inch 2117 rivets.
NR = Not Recorded.
† Lives in parentheses are those prior to refurbishment.
A/N strip = Anchor Nut strip

TABLE 5

Summary of Average Lives

	Table 4	Specimen type	Log. average life (flights)	Ratio
(1)	(a)	Control (8 mm hole)	19,250	
(2)	(b)	Boeing cold-expanded (8 mm hole)	43,376	(2)/(1) = 2·25
(3)	(c)	Boeing cold-expanded (8·71 mm hole)	39,582	(3)/(1) = 2·06 (3)/(2) = 0·92
(4)	(d)	Low-alloy steel bush (8·71 mm)	39,092	(4)/(1) = 2·03 (4)/(3) = 0·99
(5)	(e)	Low-alloy steel bush (11 mm)	47,165	(5)/(1) = 2·45 (5)/(4) = 1·21
(6)	(f)	316 stainless steel bush (11 mm)	56,704	(6)/(1) = 2·95 (6)/(5) = 1·20
(7)	(g)	Low-alloy steel bush (13 mm)	50,943	(7)/(1) = 2·65 (7)/(5) = 1·08 (7)/(4) = 1·30
(8)	(h)	316/304 stainless steel bush (13 mm)	51,096	(8)/(1) = 2·65 (8)/(7) = 1·00 (8)/(6) = 0·90

TABLE 6

Comparison of Eddy Current NDI and Fractographic Crack Measurements

Specimen			Crack details					
			Eddy Current NDI			Fractography		
No. GJ	Type	Hole No.	Position and number	Distance (and total length) in mm‡	Max. signal height (%)	Position and number	Distance (and total length) in mm‡	Max. depth (mm)
2B15	Bushed (8·71 mm)	1	Inner 1 2 3	0–2 (2) 10–21 (11) 21–23 (2)	20 40 20	Inner 1 2	3·85–6·13 (2·28) 11·57–20·44 (8·87)	0·81 3·71
			Outer 1	17–23 (6)	30	Outer 1 2	14·54–15·95 (1·41) 16·24–21·08 (4·84) Overall distance 1+2 = 6·54	0·39 1·95
2B4	Bushed (11 mm)	1	Inner No cracks detected			Inner Seven small cracks ranging from 0·52 to 1·86 mm in length and 0·14 to 0·38 mm in depth		
			Outer 1	0–6 (6)	30	Outer 1	0·54–4·60 (4·06)	1·87
2B3	Bushed (11 mm)	1	Inner 1	2·5–4·5 (2)	30	Inner 1 2	1·33–1·57 (0·24) 1·81–3·52 (1·71) Overall distance 1+2 = 2·19	0·38 0·66
		1	Inner 3	9–22 (13)	60	Inner 3	10·56–20·84 (10·28)	4·51
		3	Inner 1	6–23 (17)	50	Inner 1	7·06–23·0 (15·94)	7·32*
			* Maximum depth measured. Boundary of crack lost during cutting of specimen					

TABLE 6 (Continued)

Specimen			Crack details					
			Eddy Current NDI			Fractography		
No. GJ	Type	Hole No.	Position and number	Distance (and total length) in mm	Max. signal height (%)	Position and number	Distance (and total length) in mm	Max. depth (mm)
2B12	Bushed (11 mm)	1	Outer 1	0–13 (13)	60	Fracture surfaces not examined		
2A9	Bushed (11 mm)	3	Inner 1	0–6 (6)	90	Inner 1 2	0–3·19 (3·19) 3·85–4·17 (0·32) Overall distance 1+2 = 4·17	(surface) 6·92 0·10
2A5	Bushed (13 mm)	1	Outer 1	5·5–11 (5·5)	20	Fracture surfaces not examined		
2A13	Bushed (13 mm)	3	Inner 1	0–8·5 (8·5)	30	Inner 1	0–8·64 (8·64)	(See Fig. 15) 14·93

‡ Distances measured from 'Skin' face—Datum Face 'C'.

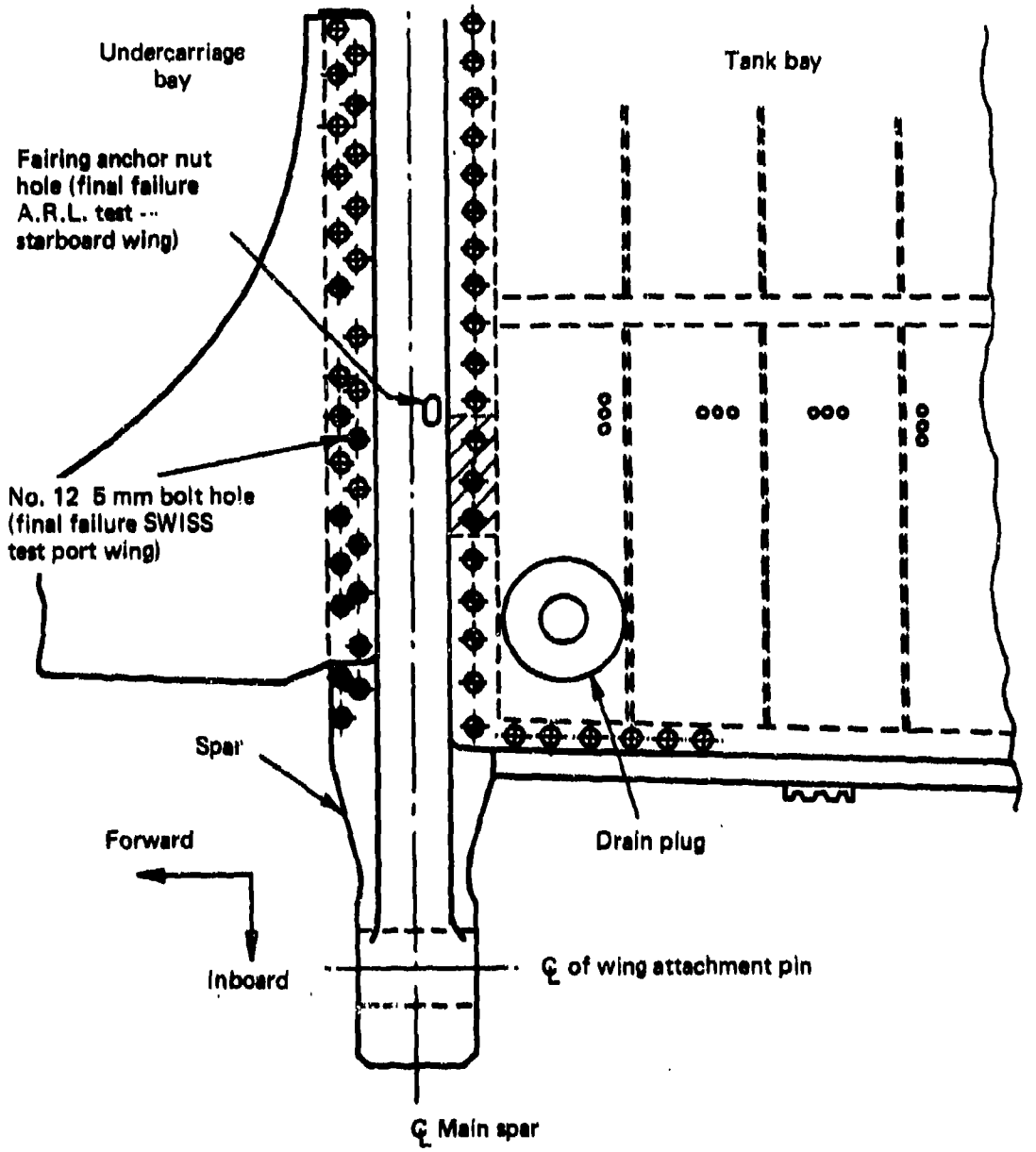

⊕	10 mm	hex.head shoulder bolt
⊕	8 mm	hex.head shoulder bolt
⊕	8 mm	countersunk head screw
⊕	6 mm	countersunk head screw
⊕	5 mm	hex.head bolt
⊕	5 mm	countersunk head bolt
⊕	Rivet	

Region of structure covered by this investigation

FIG. 1 MIRAGE PORT WING VIEWED FROM LOWER SURFACE

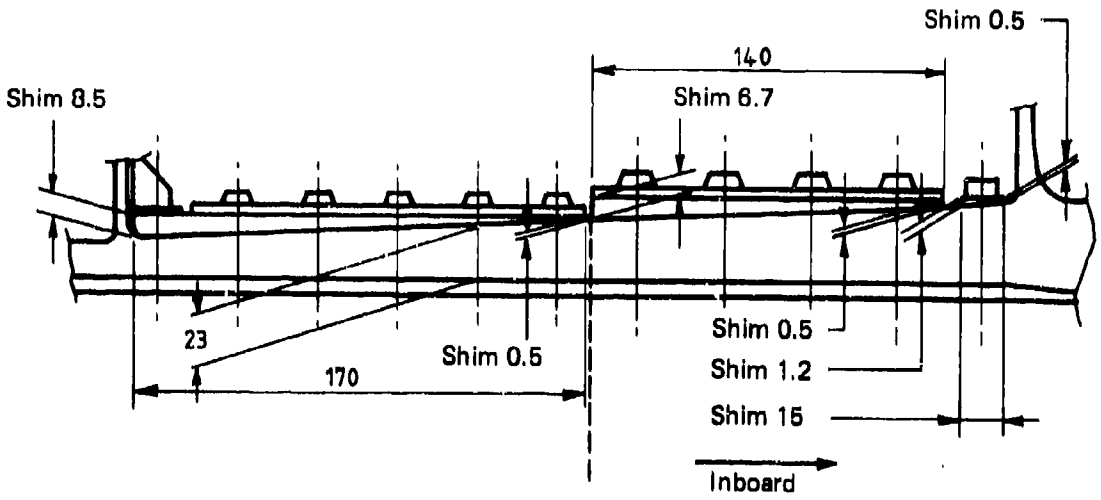

Legend

- 10 mm dia. shoulder bolt (8 x 1.25 thread)
- 8 mm dia. shoulder bolt (6 x 1 thread)
- 3 mm dia. c sunk head rivet (A-U4G)
- 2.5 mm dia. c sunk head rivet (A-U4G)

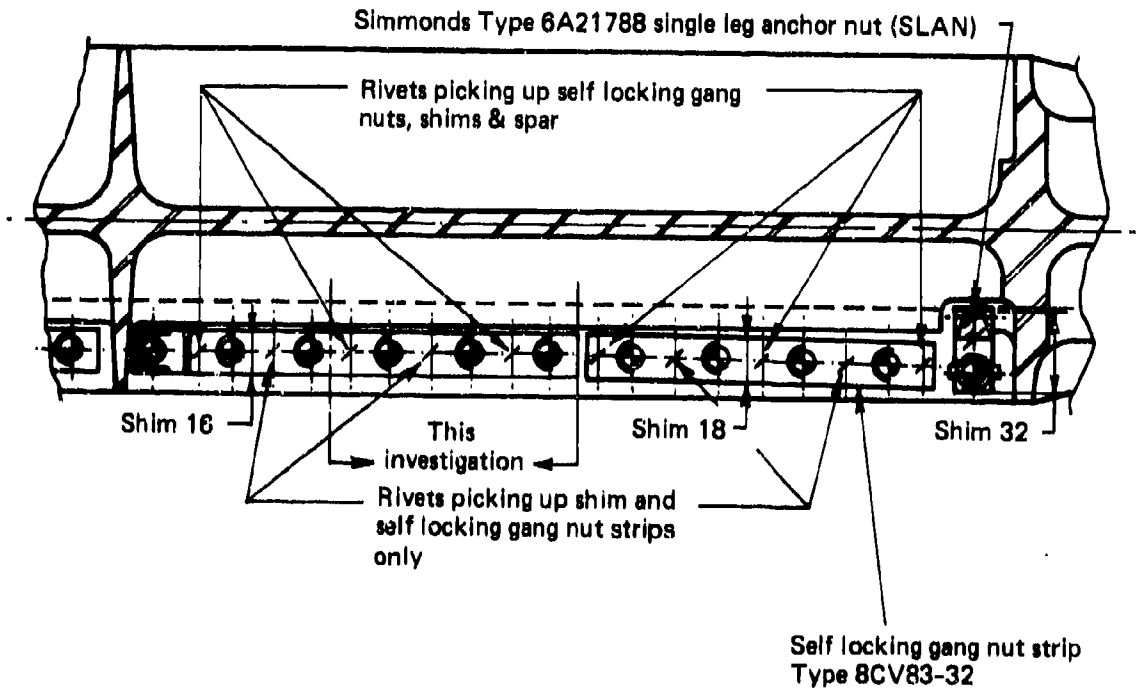

All dimensions in mm

Taken from AMD Manufacturing Drawing No. MIR.IIIE-113/2

FIG. 2 MAIN SPAR LOWER SURFACE, REAR FLANGE DETAIL

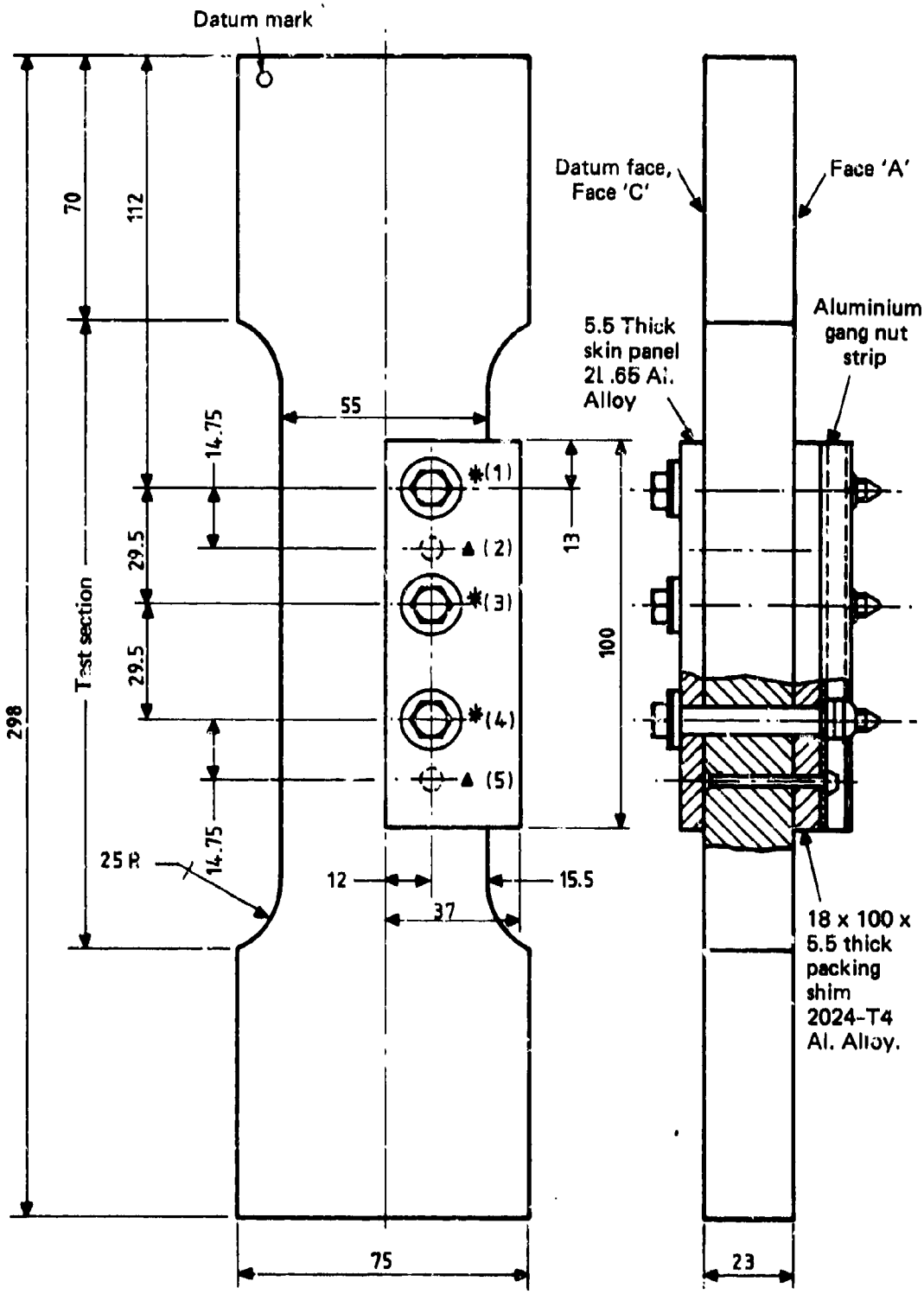

▲ 3.0 Dia. A-U4G rivet

✱ 8.0 Dia. shoulder bolts (6.0 dia. thread)

Rivet/bolt position indicated by number in ( )

All dimensions in mm

material: 2014-T651 Al. Alloy

FIG. 3 MIRAGE SPAR – LOWER REAR FLANGE SECOND GANG NUT STRIP FATIGUE SPECIMEN

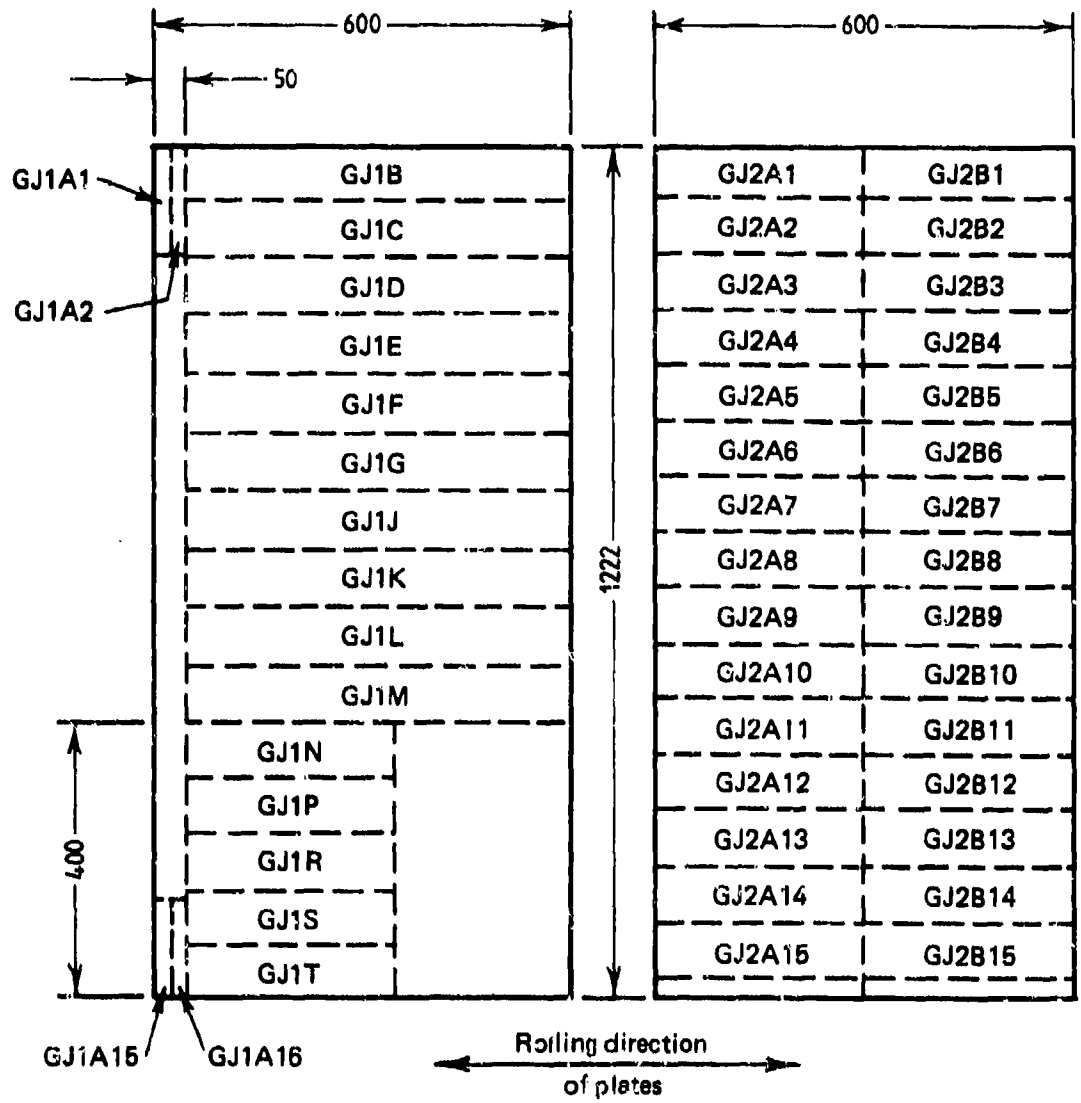

Test material:

2014-T651 Aluminium alloy bare plate, thickness 1.260 inch (32 mm), manufactured to specification QQ-A-255 by Kaiser Aluminium USA.

Static tension specimens: GJ1A1, GJ1A2, GJ1A15, GJ1A16
Fatigue specimens (this investigation): GJ1N – GJ1T, GJ2A1 – GJ2A15, GJ2B1 – GJ2B15.

FIG. 4 FATIGUE SPECIMEN POSITIONS IN PLATE SERIAL NO. GJ

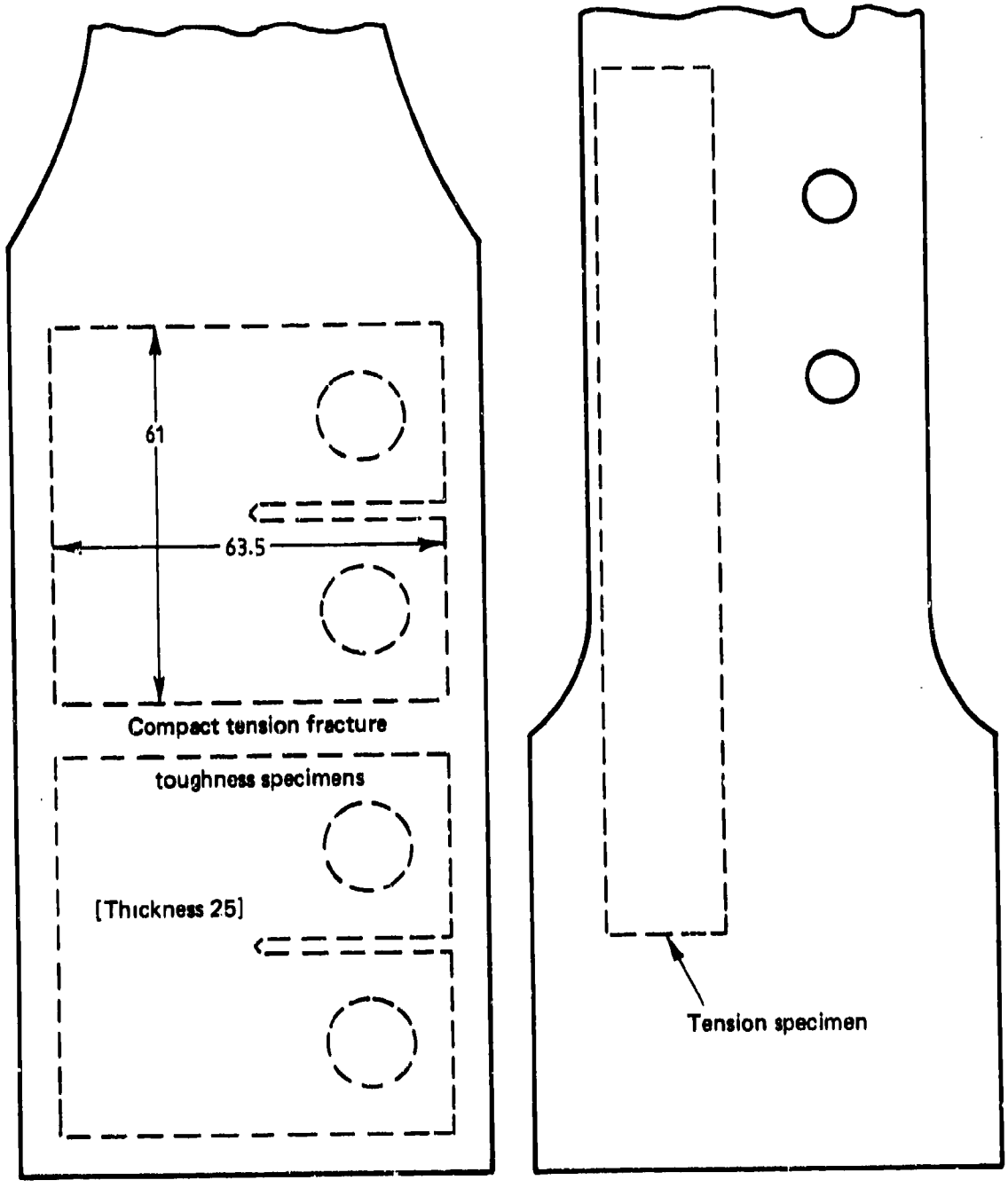

FIG. 5 LOCATIONS OF FRACTURE TOUGHNESS AND TENSION SPECIMENS

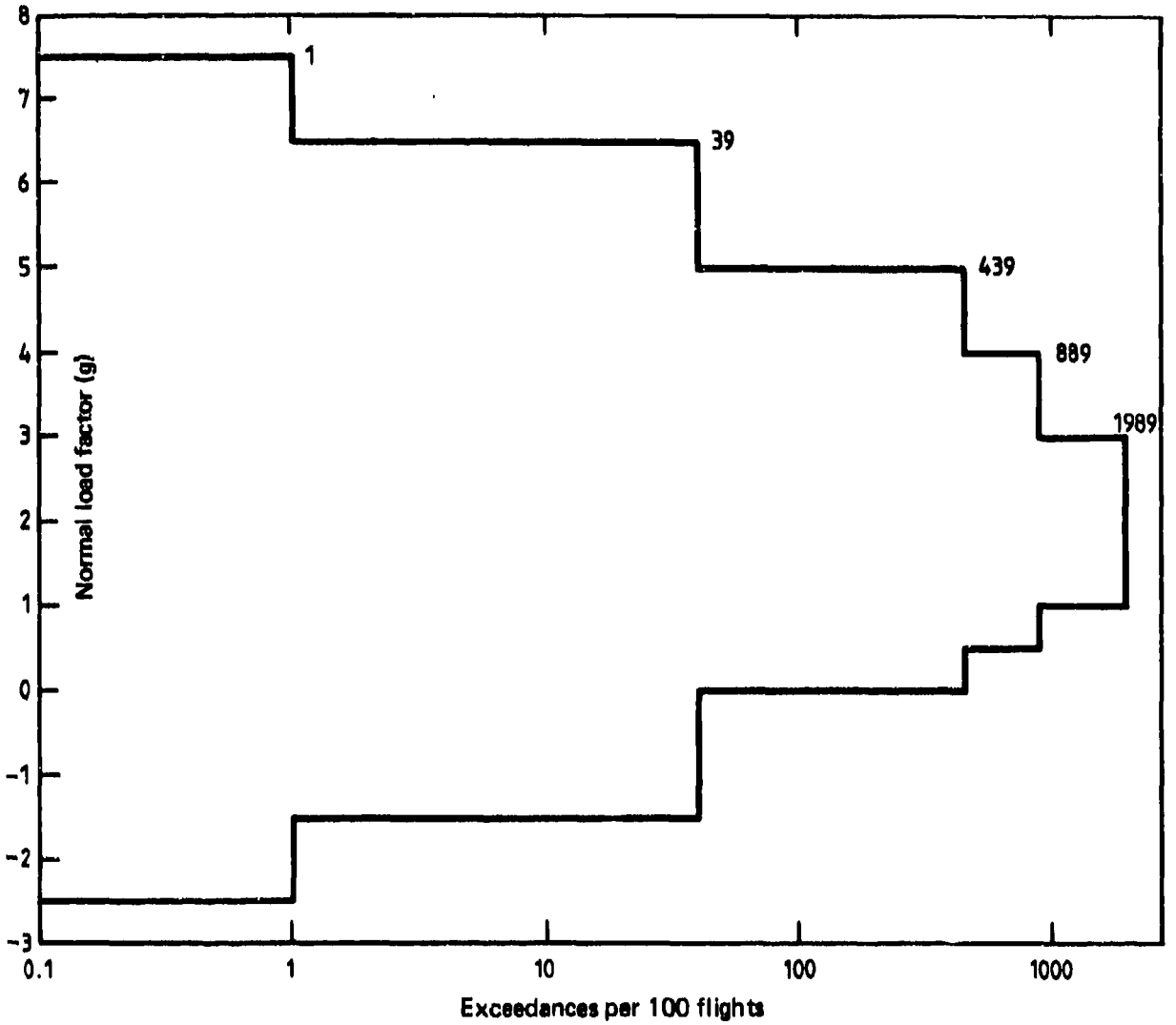

FIG. 6 TEST LOADING SPECTRUM FOR 100 FLIGHTS

100 FLIGHTS (1989 CYCLES) REPRESENT 66.6 HOURS OF FLYING

FLIGHT A' →	10 CYCLES +3g/+1g	5 CYCLES +4g/+0.5g	2 C[illegible] +5[illegible]	1 CYCLE +6.5g/-1.5g	1 CYCLE +7.5g/-2.5g	1 CYCLE +6.5g/-1.5g	2 CYCLES +5g/0g	4 CYCLES +4g/+0.5g	10 CYCLES +3g/+1g
FLIGHT A →	10 CYCLES +3g/+1g	2 CYCLES +4g/+0.5g	2 CYCLES +5g/0g	2 CYCLES +6.5g/-1.5g	2 CYCLES +5g/0g	2 CYCLES +4g/+0.5g	5 CYCLES +3g/+1g		
FLIGHT B →	5 CYCLES +3g/+1g	5 CYCLES +4g/+0.5g	9 CYCLES +5g/0g	4 CYCLES +4g/+0.5g	5 CYCLES +3g/+1g				
FLIGHT C →	5 CYCLES +3g/+1g	1 CYCLE +4g/+0.5g	5 CYCLES +3g/+1g						

CYCLES OF +6.5g/-1.5g AND +7.5g/-2.5g AT 1 Hz;
REMAINDER OF CYCLES AT 3 Hz

SEQUENCE OF FLIGHTS IN 100 FLIGHTS: 1 FLIGHT A', 18 FLIGHTS A, 36 FLIGHTS B AND 45 FLIGHTS C

1	2	3	4	5	6	7	8	9	10	11	12	13	14	15	16	17	18	19	20	21	22	23	24	25
B	C	C	B	C	C	C	A	C	C	B	B	A	C	C	C	B	A	C	B	B	B	A	C	C
51	52	53	54	55	56	57	58	59	60	61	62	63	64	65	66	67	68	69	70	71	72	73	74	75
C	B	C	C	B	C	B	B	C	C	C	A	B	A	C	C	C	B	A	B	B	B	C	B	C

26	27	28	29	30	31	32	33	34	35	36	37	38	39	40	41	42	43	44	45	46	47	48	49	50
C	A	A	C	C	B	B	B	C	B	A	B	C	C	B	A	[illegible]	B	C	C	A	A	B	B	C
76	77	78	79	80	81	82	83	84	85	86	87	88	89	90	91	[illegible]	93	94	95	96	97	98	99	100
C	A	B	C	B	A	B	C	C	B	A	A	B	C	C	B	C	C	B	B	C	B	C	A	C

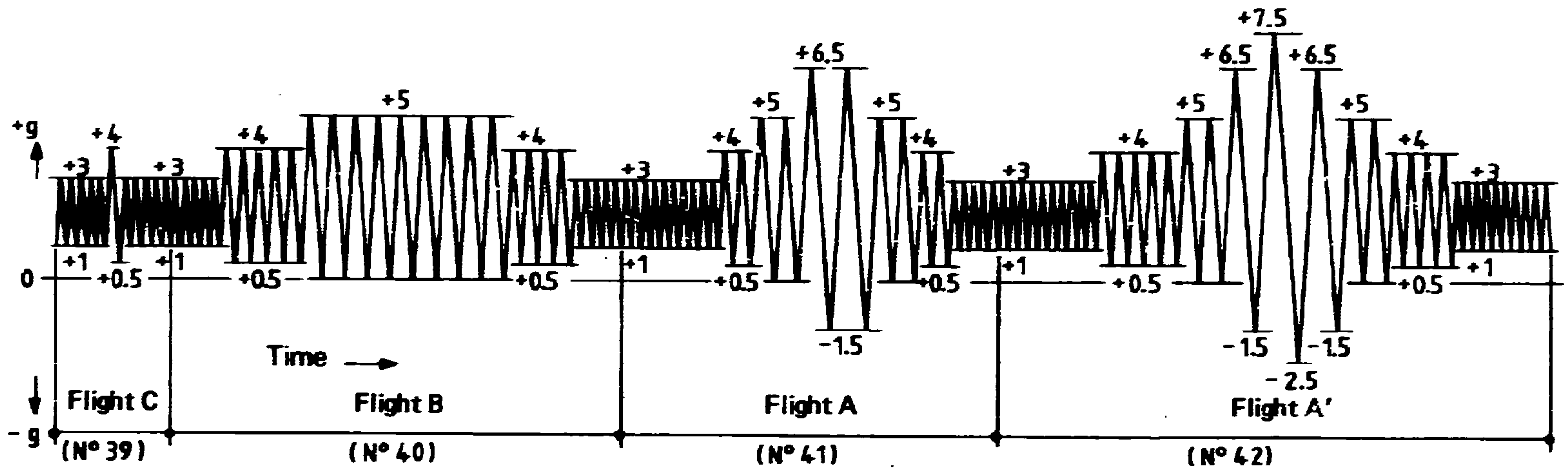

FIG. 7 FRENCH 100 FLIGHT MIRAGE 111 FLIGHT-BY-FLIGHT SEQUENCE

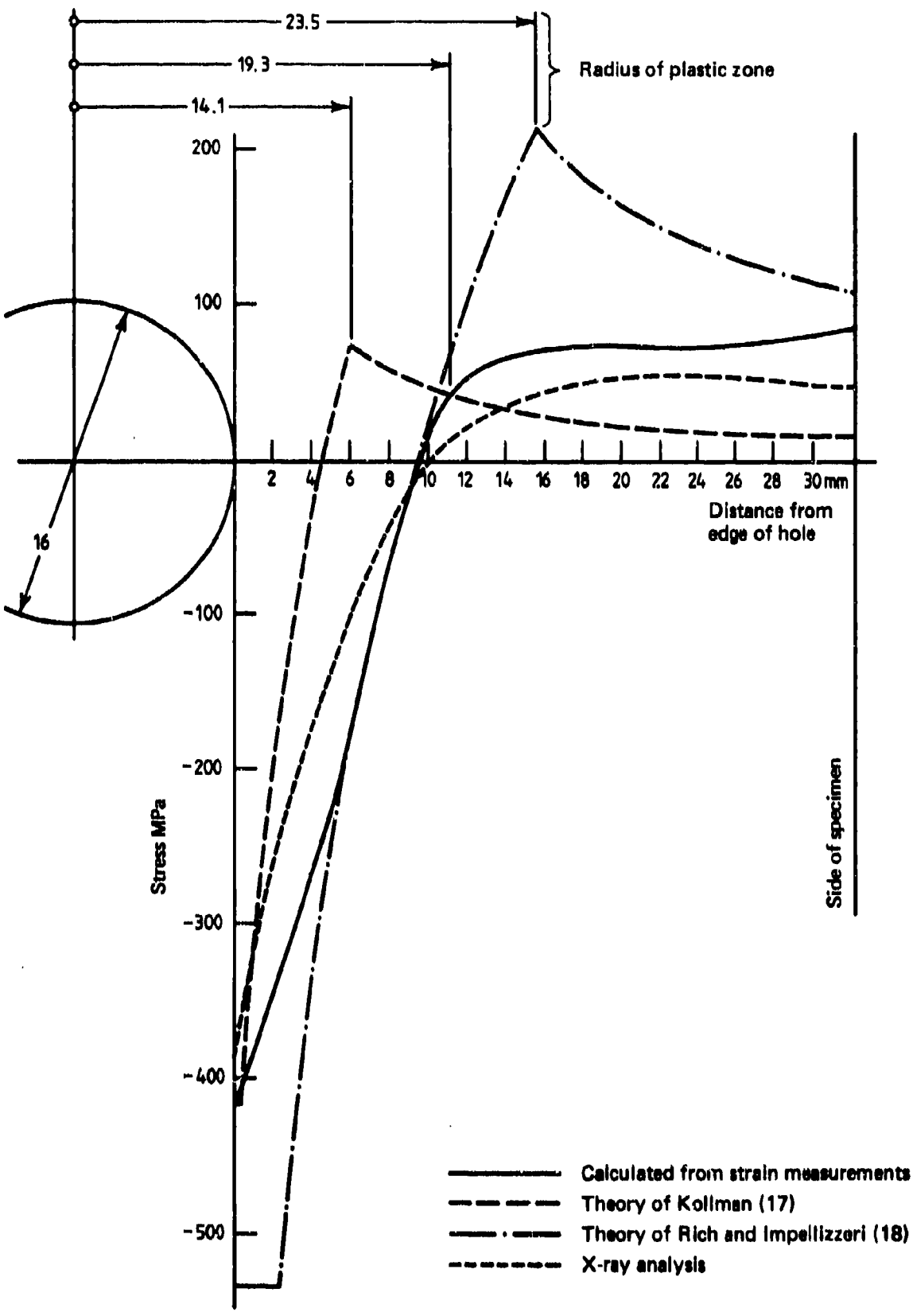

FIG. 8 COMPARISON OF CALCULATED AND MEASURED RESIDUAL HOOP STRESS DISTRIBUTIONS FOR 4.5% COLD-EXPANDED HOLE IN 10 mm THICK ALUMINIUM ALLOY PLATE (16).

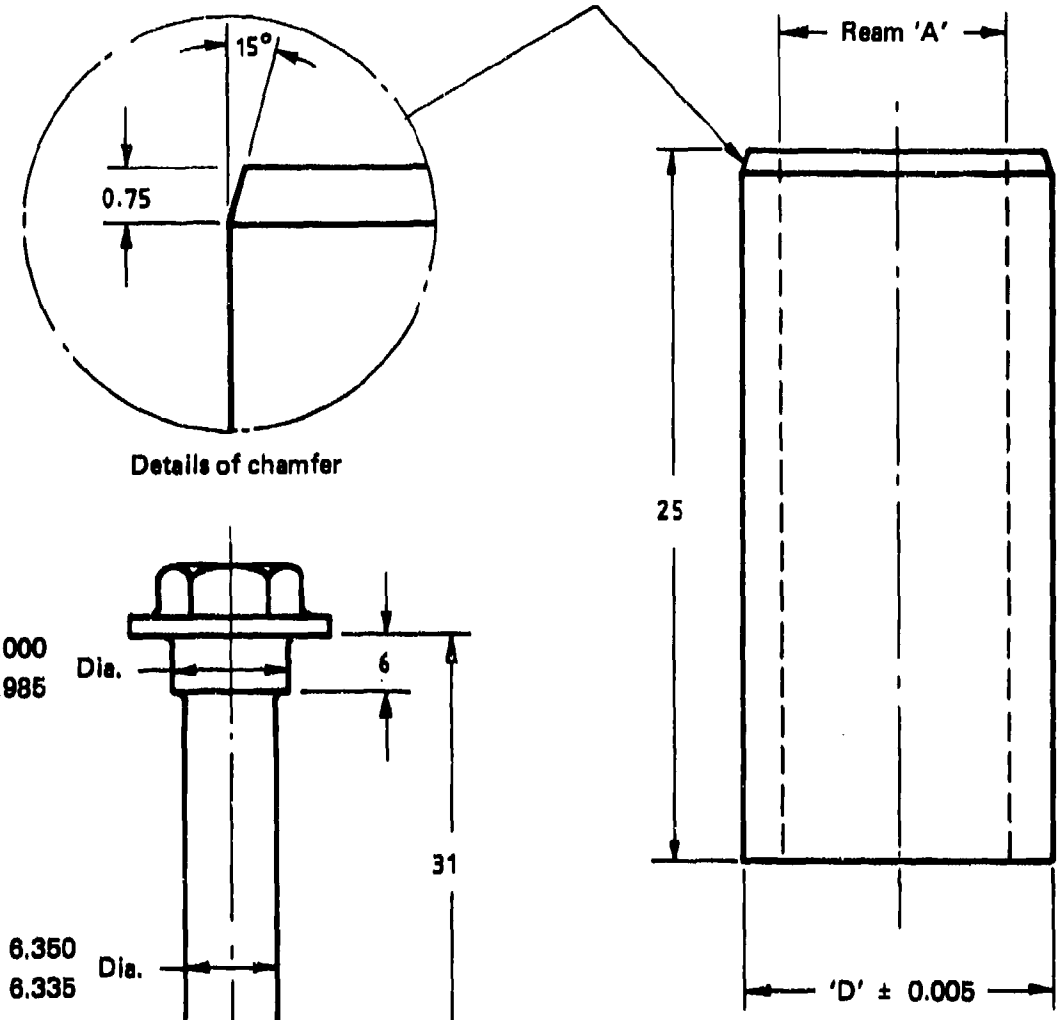

Bore 'A'	
Std Bolt	U/size bolt
8.035 8.013	6.385 6.363

Notes

1. Diameter 'D' to be 0.25 to 0.35% greater than measured hole diameter
2. Material to be as specified
3. External surfaces to be ground finish
4. All dimensions in mm

FIG. 9 STEEL BUSHES AND STEPPED BOLT

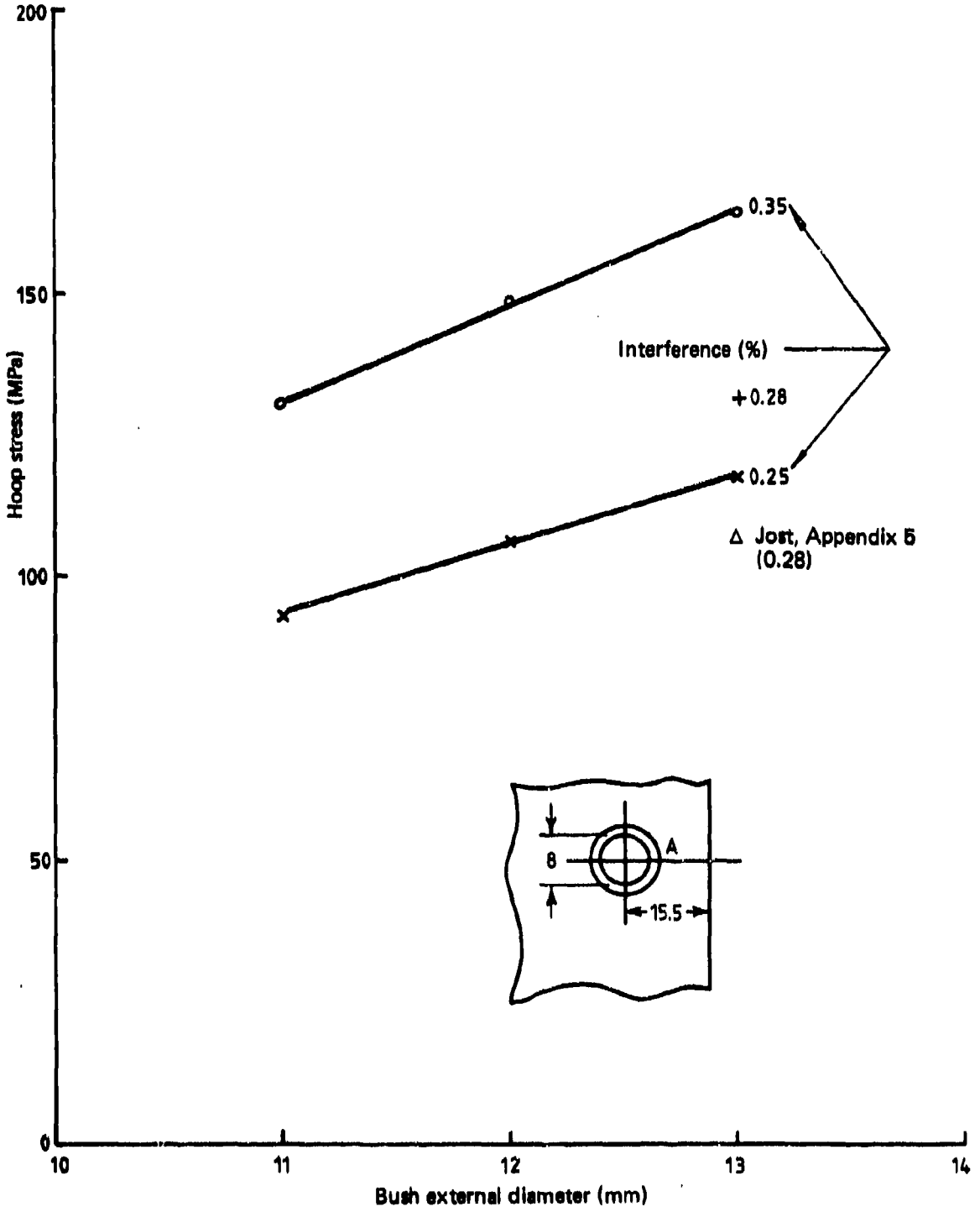

FIG. 10 HOOP STRESSES INDUCED ON HOLE SURFACE AT 'A' BY STEEL BUSHES OF 8 mm INTERNAL DIAMETER (34)

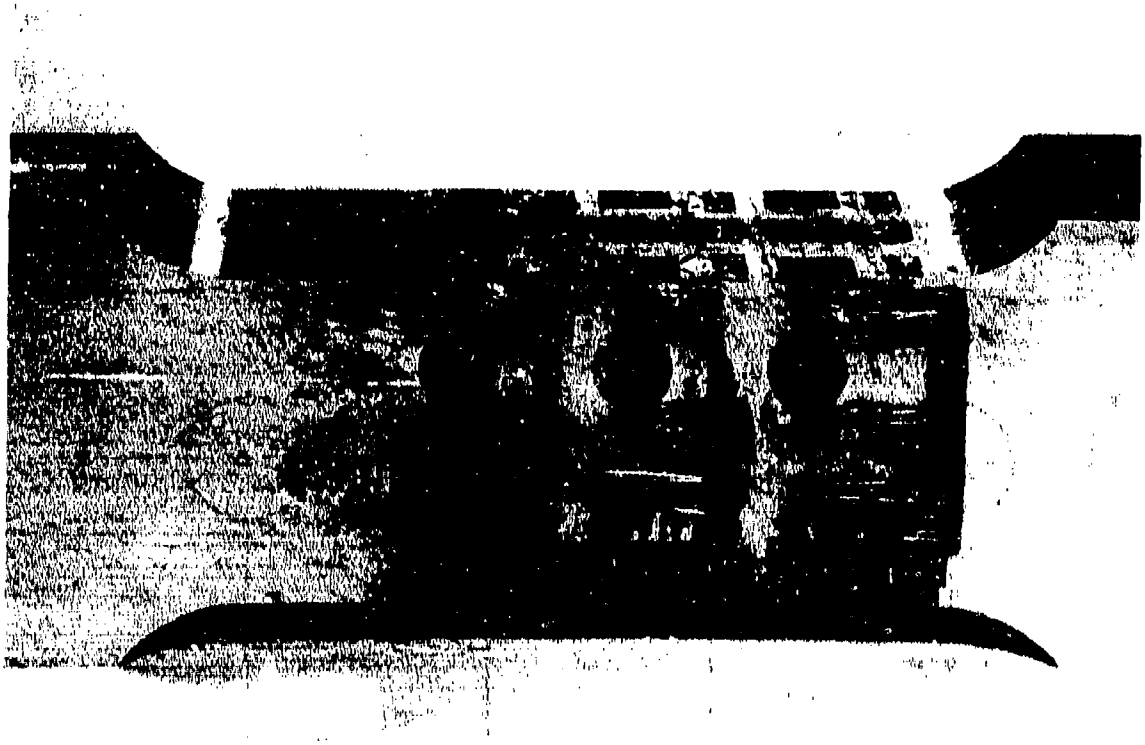

Underneath face

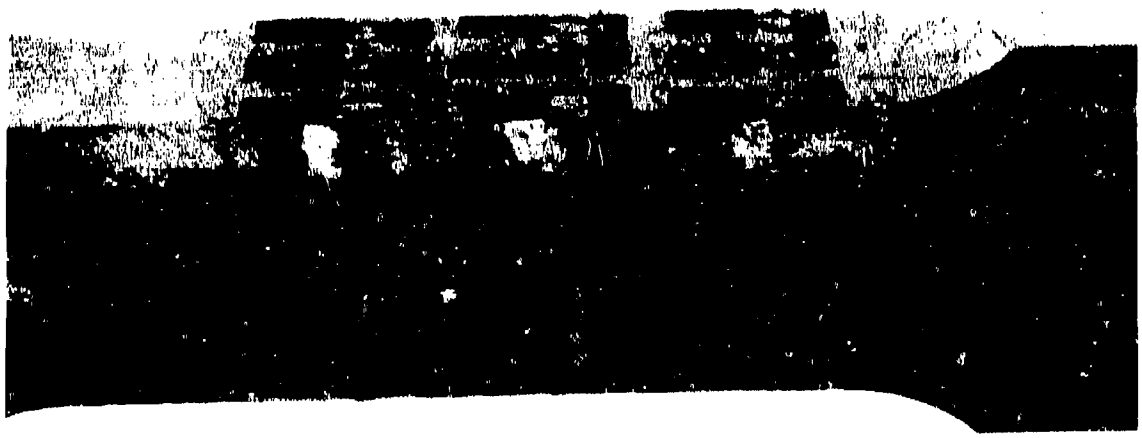

FIG. 11 STRAIN GAUGE POSITIONS ADJACENT TO BUSHED HOLES

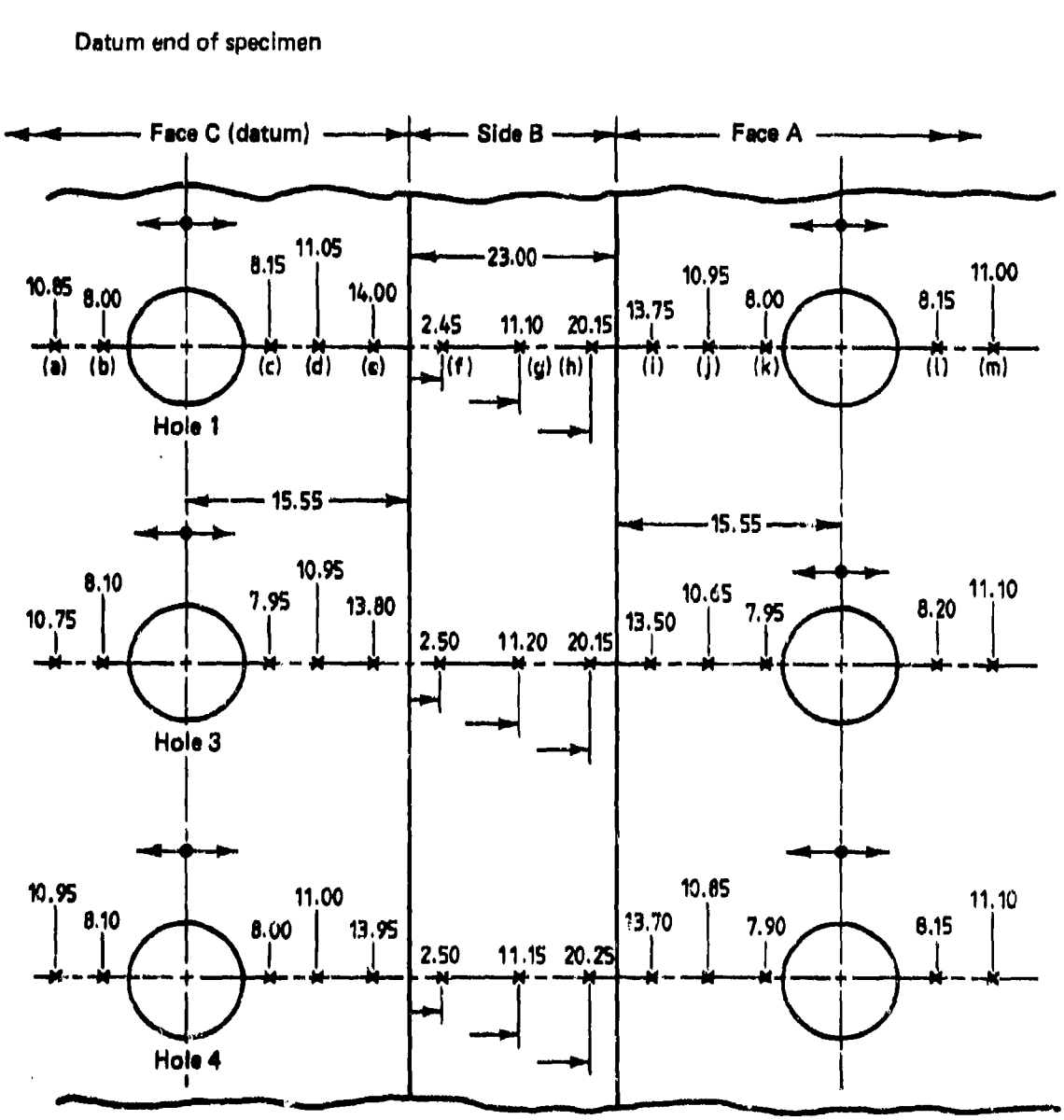

Note:

Dimensions in millimetres (to nearest 0.05 mm).
Gauges on Faces A and C = 3 mm long x 1 mm wide.
Gauges on Side B = 6 mm long x 2 mm wide.
All holes nominally 13 mm diameter.

FIG. 12 DETAILS OF STRAIN GAUGE POSITIONS ON SPECIMEN GJ2A15

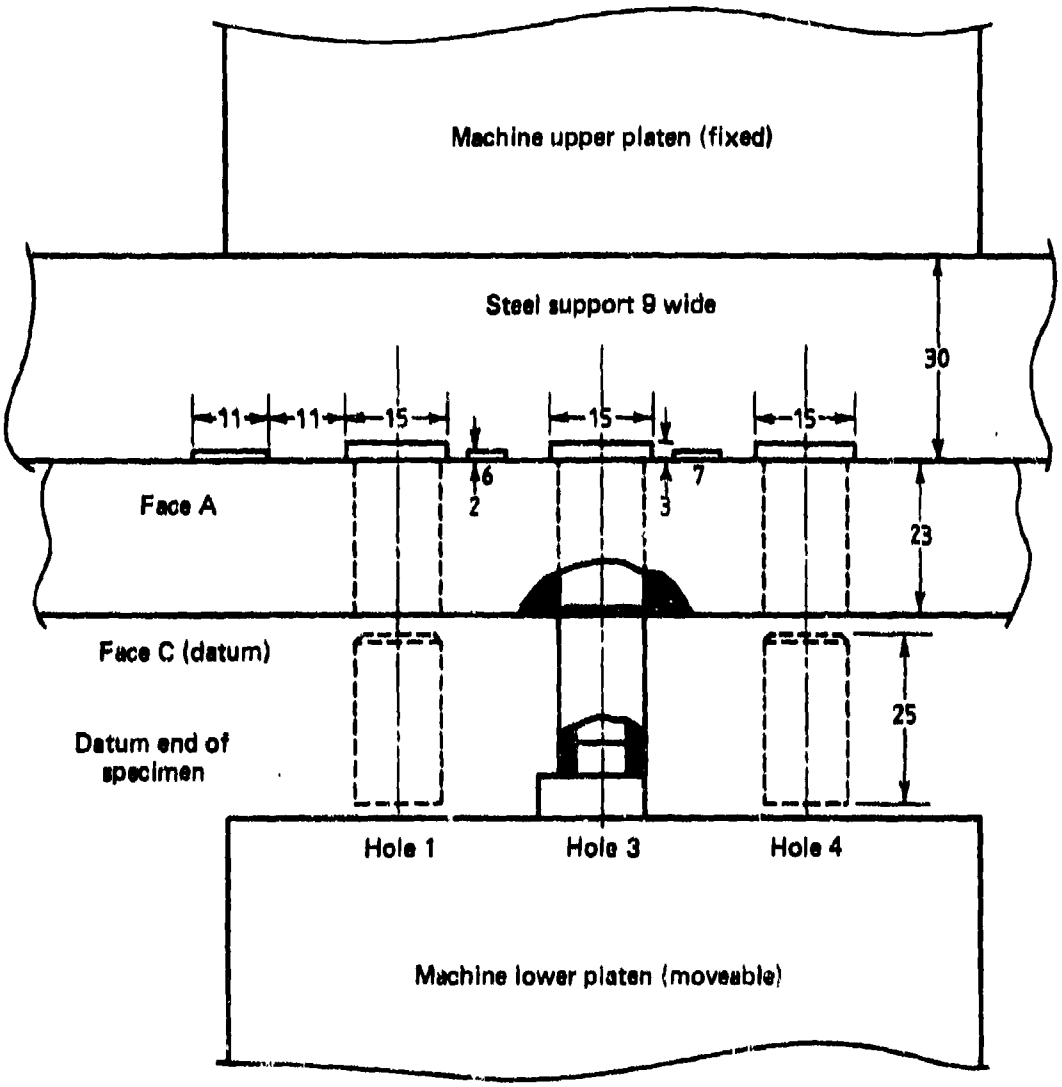

Dimensions in millimetres.
2 and 3 mm grooves to accommodate strain gauge leads and provide clearance for bushes

FIG. 13 SET-UP FOR BUSH INSERTION IN STRAIN-GAUGED SPECIMEN

Spec. No. GJ
2A2
Type:
Control

Flights: 13,842
Failure at
Hole 1

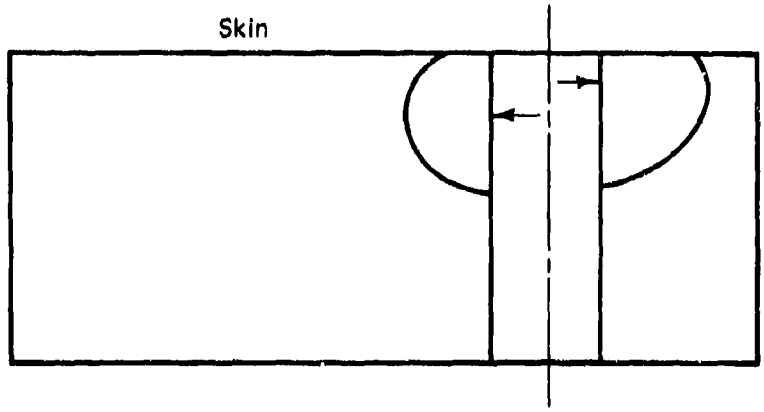

Spec. No. GJ
1R
Type:
Control

Flights: 14,025
Failure at
Hole 1

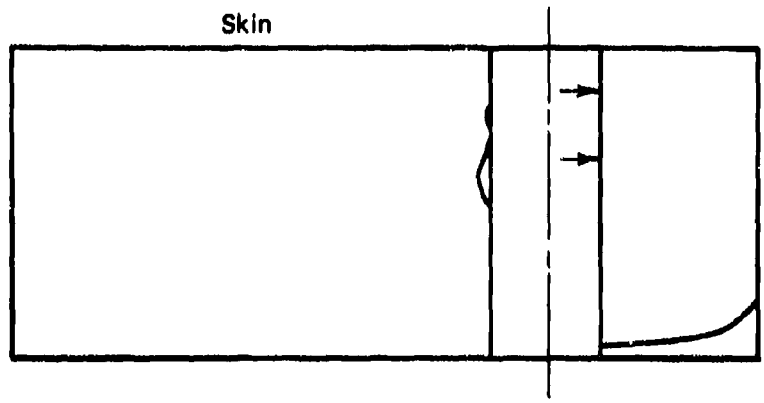

Spec. No. GJ
2B5
Type:
Control

Flights: 18,190
Failure at
Hole 1

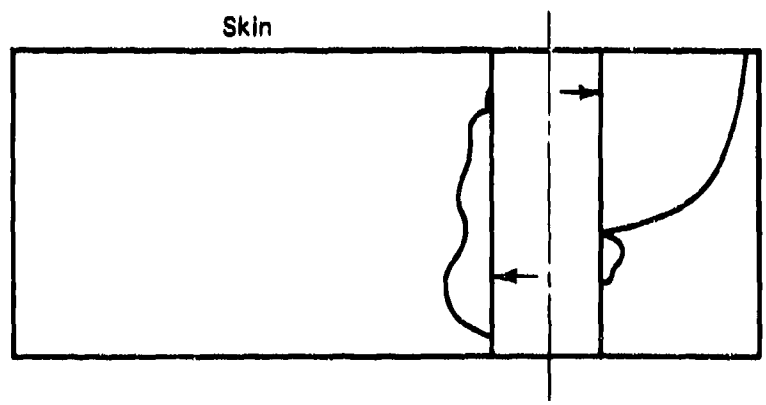

Spec. No. GJ
2A14
Type:
Control

Flights: 26,042
Failure at
Hole 1

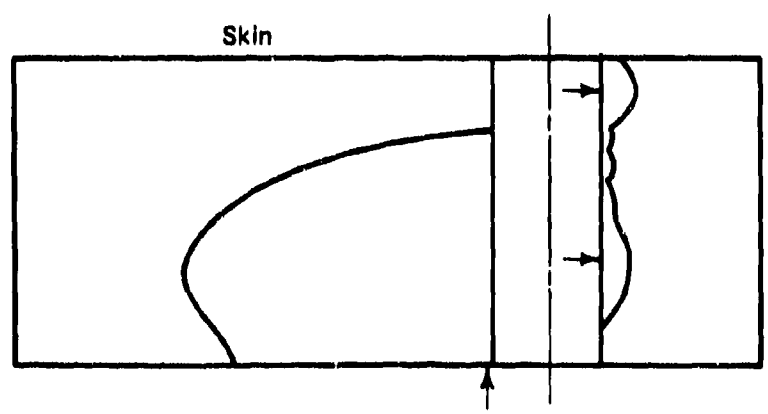

FIG. 14(a) FATIGUE-CRACKED AREAS

(Arrows denote major fatigue crack initiation points)

Spec. No. GJ
2B11
Type:
Control

Flights: 28,742
Failure at
Hole 4

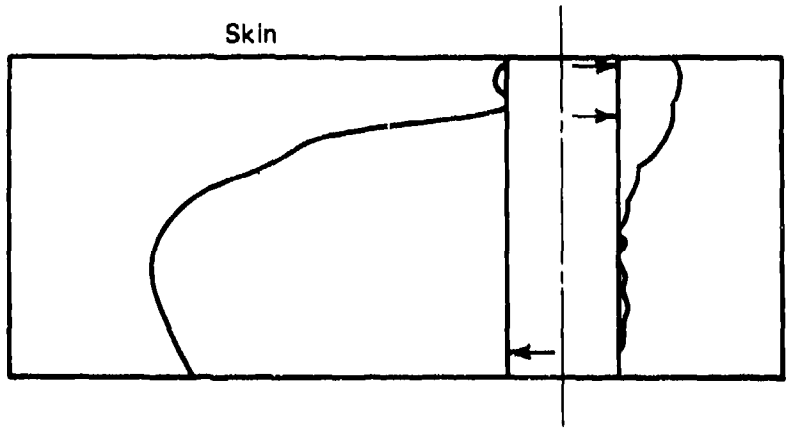

Spec. No. GJ
2A6
Type: Non-assembled

Flights: 13,542
Failure at
Hole 1

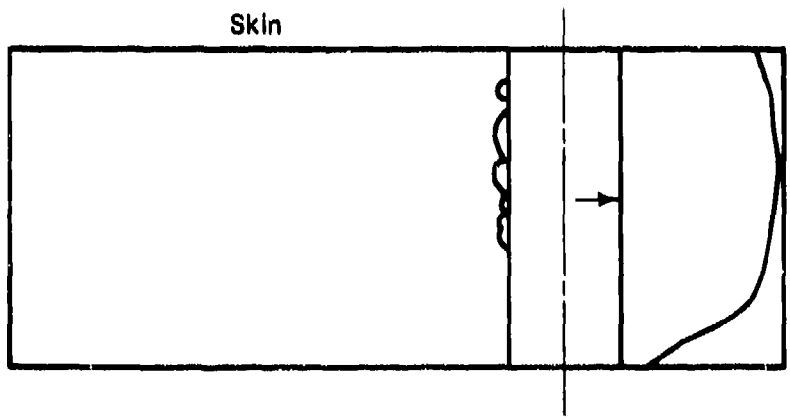

FIG. 14(b) FATIGUE-CRACKED AREAS

Spec. No. GJ
1T
Type: 8 mm
Cold-expanded
Flights: 33,742
Failure at
Hole 4

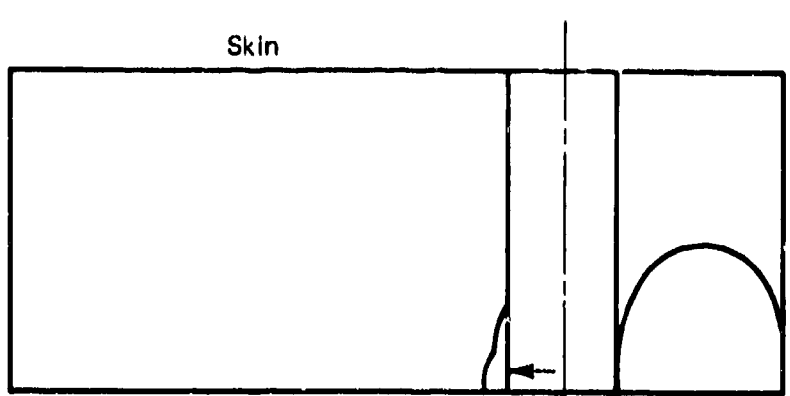

Spec. No. GJ
1N
Type: 8 mm
Cold-expanded
Flights: 42,442
Failure at
Hole 4

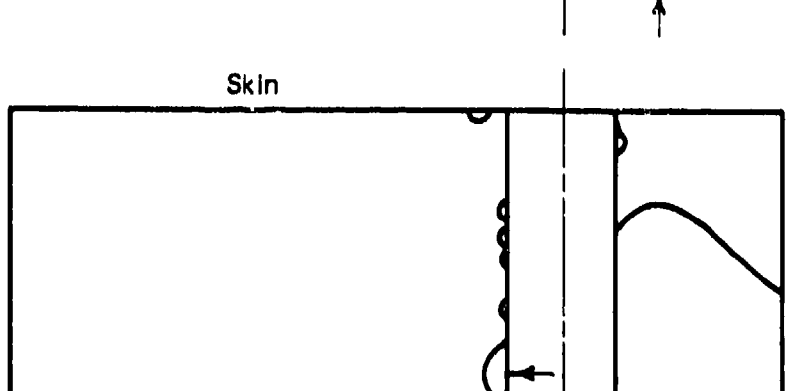

Spec. No. GJ
1P
Type: 8 mm
Cold-expanded
Flights: 48,642
Failure at
Hole 4

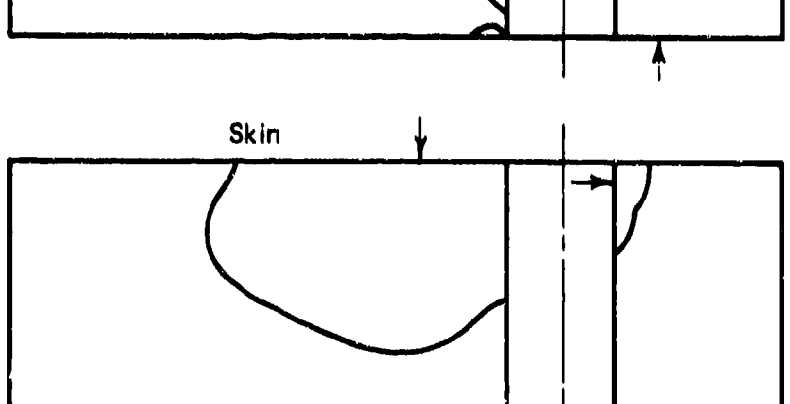

Spec. No. GJ
1S
Type: 8 mm
Cold-expanded
Flights: 50, 817
Failure at
Hole 1

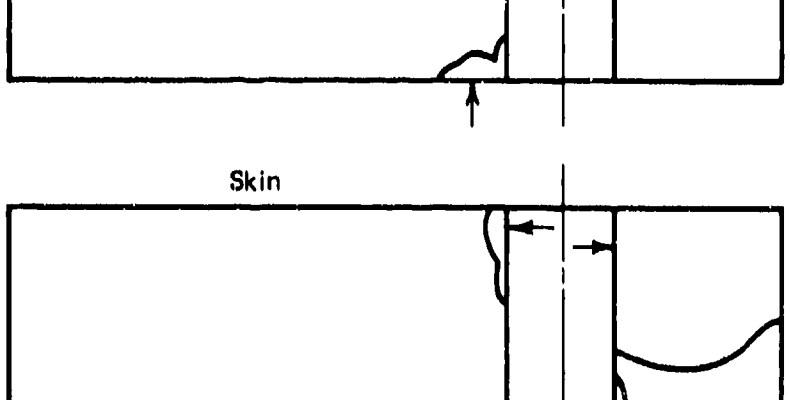

FIG. 14(c) FATIGUE-CRACKED AREAS

Spec. No. GJ
289
Type: 8.71 mm
Cold-expanded

Flights: 35,342
Failure at
Hole 4

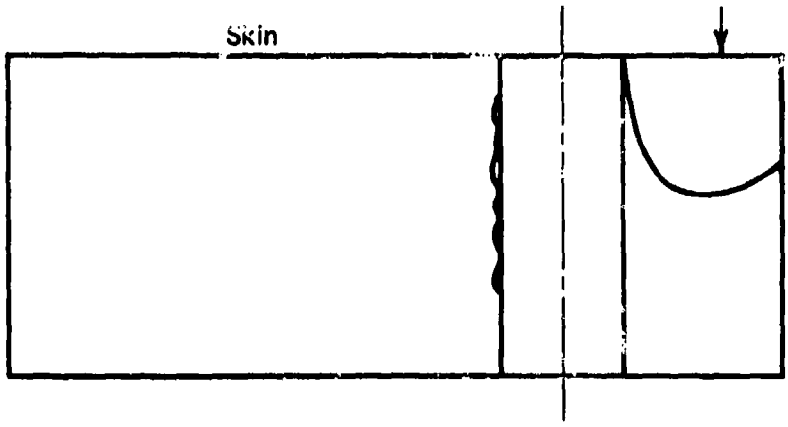

Spec. No. GJ
2A10
Type: 8.71 mm
Cold-expanded

Flights: 41,342
Failure at
Hole 4

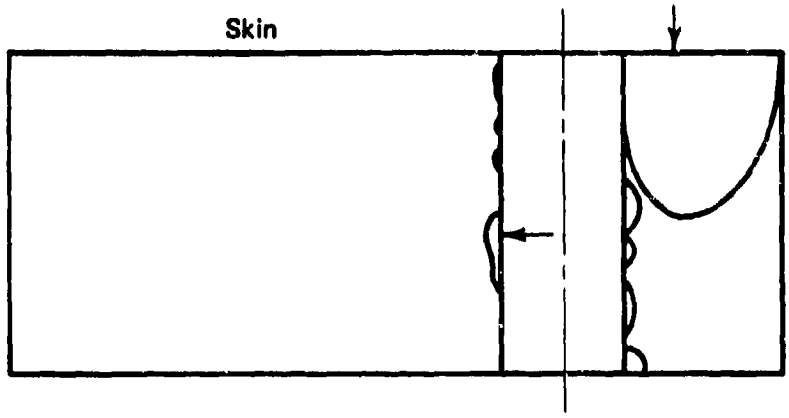

Spec. No. GJ
2B6
Type: 8.71 mm
Cold-expanded

Flights: 42,442
Failure at
Hole 4

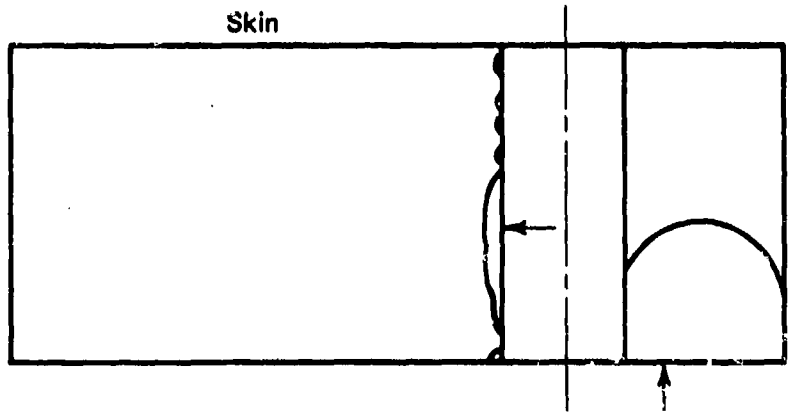

FIG. 14(d) FATIGUE-CRACKED AREAS

Spec. No. GJ
2A3
Type: 8.71 mm
LAS bush

Flights: 37,500
Failure at
Hole 5

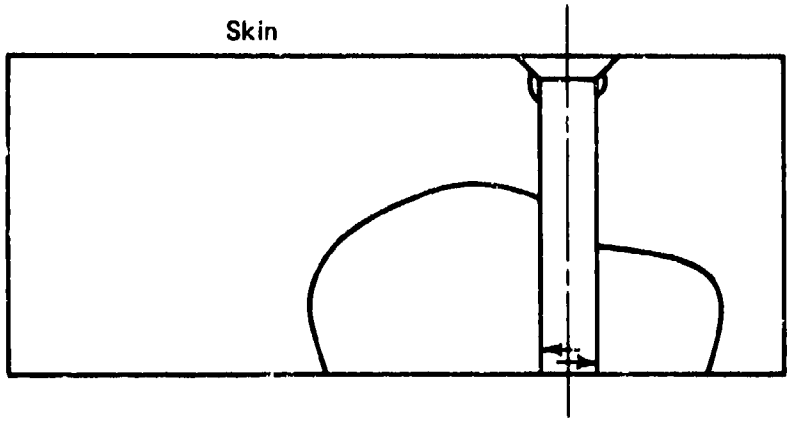

Spec. No. GJ
2A11
Type: 8.71 mm
LAS bush

Flights: 39,042
Failure at
Hole 4

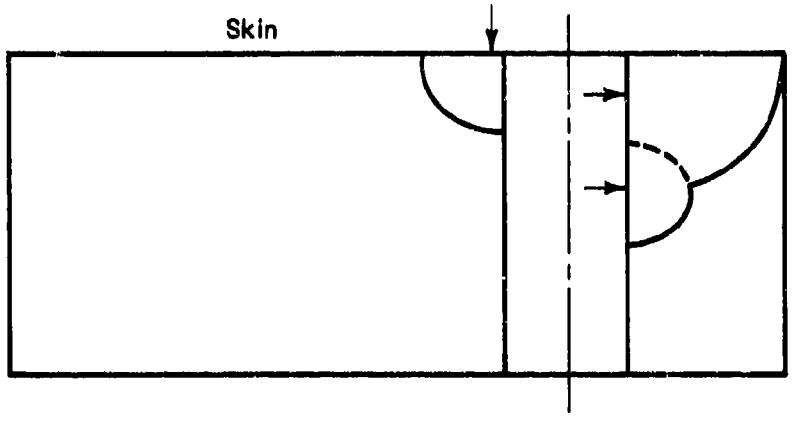

Spec. No. GJ
2B15
Type: 8.71 mm
LAS bush

Flights: 39,142
Failure at
Hole 4

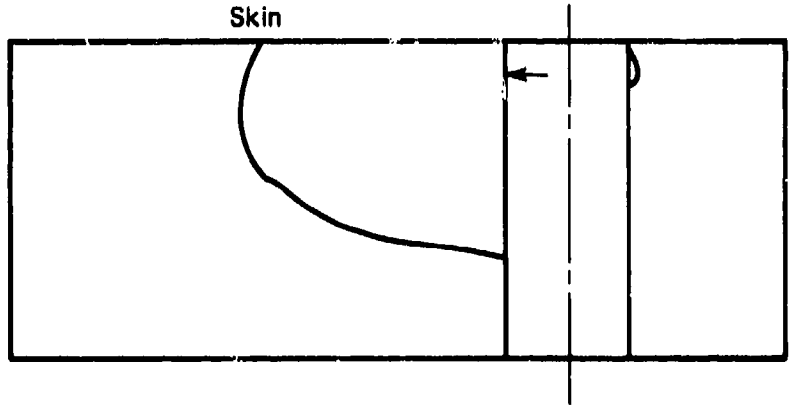

FIG. 14(e) FATIGUE-CRACKED AREAS

Spec. No. GJ
2B4
Type: 11 mm
LAS bush

Flights: 29,100
Failure at
Hole 5

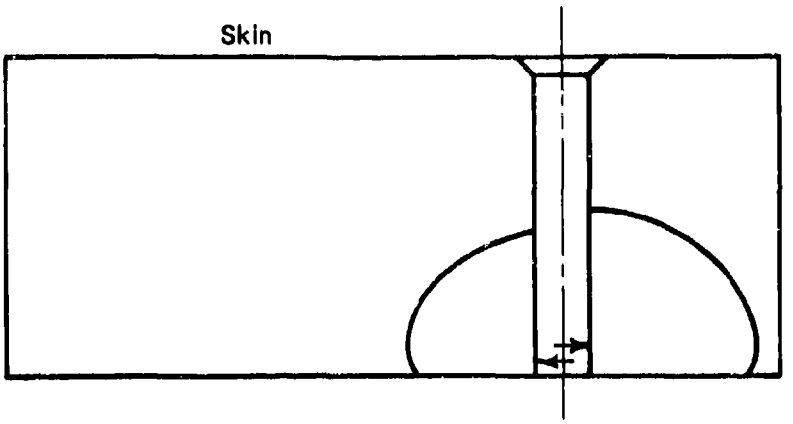

Spec. No. GJ
2B3
Type: 11 mm
LAS bush

Flights: 44,542
Failure at
Hole 4

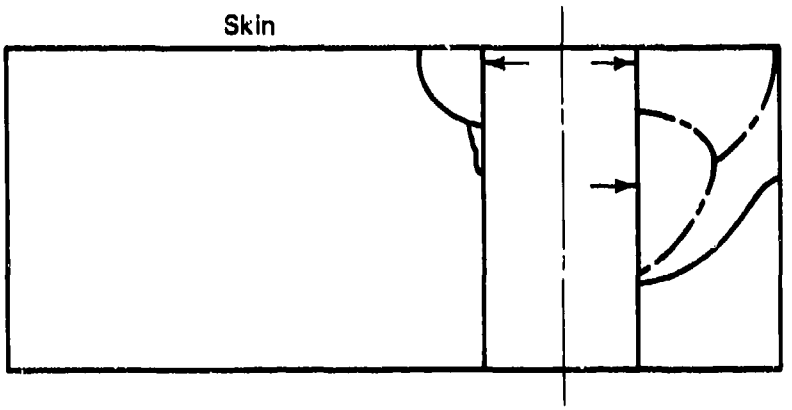

Spec. No. GJ
2B12
Type: 11 mm
LAS bush

Flights: 49,942
Failure at
Hole 4

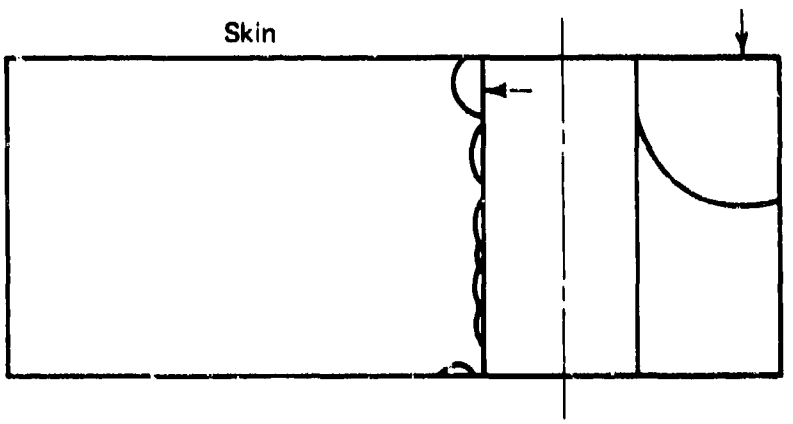

Spec. No. GJ
2A1
Type: 11 mm
316 bush

Flights: 55,842
Failure at
Hole 1

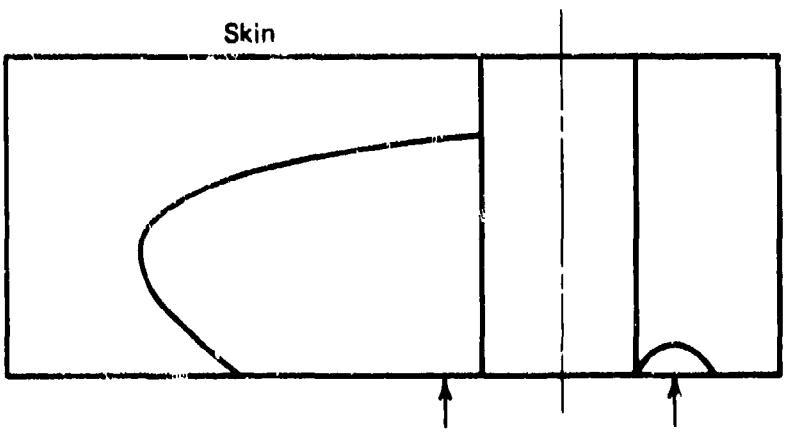

FIG. 14(f) FATIGUE-CRACKED AREAS

Spec. No. GJ
2A9
Type: 11 mm
316 bush
Flights: 57,580
Failure at
Hole 1

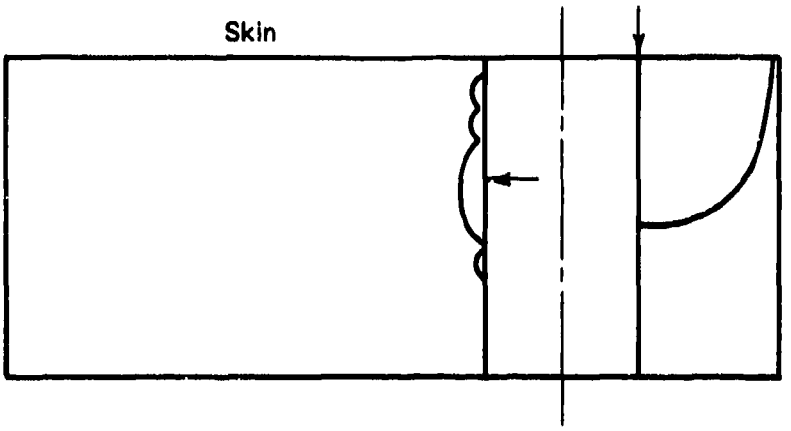

FIG. 14(g) FATIGUE-CRACKED AREAS

Spec. No. GJ
2A5
Type: 13 mm
LAS bush

Flights: 40,778
Failure at
Hole 4

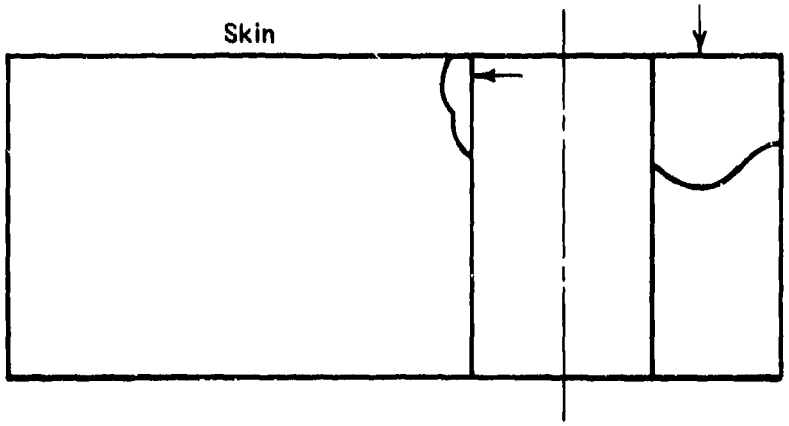

Spec. No. GJ
2B2
Type: 13 mm
LAS bush

Flights: 63,642
Failure at
Hole 4

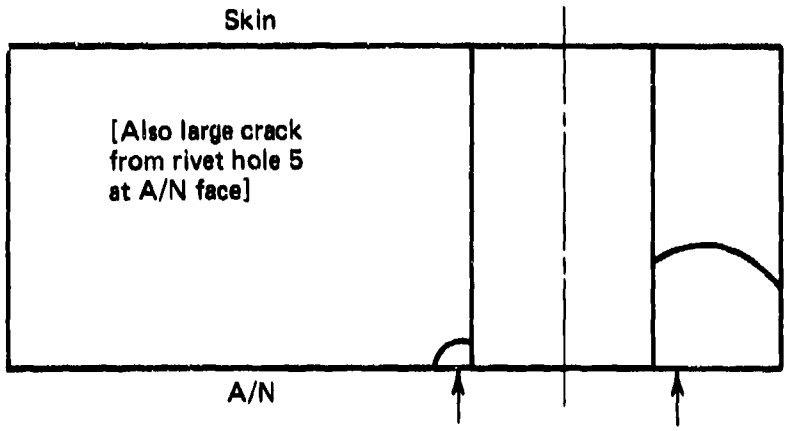

Spec. No. GJ
2A7
Type: 13 mm
316 bush

Flights: 38,200
Failure at
Hole 1

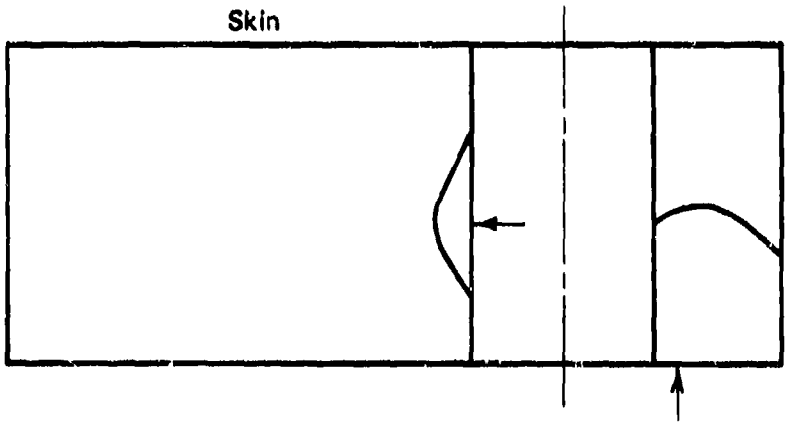

Spec. No. GJ
2B10
Type: 13 mm
316 bush

Flights: 45,442
Failure at
5

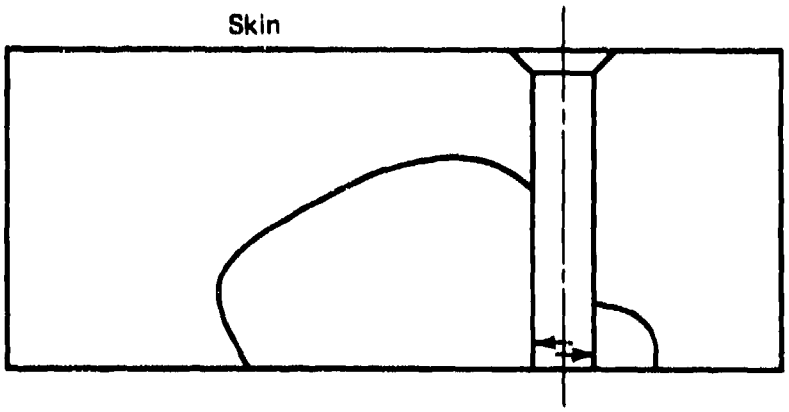

FIG. 14(h) FATIGUE-CRACKED AREAS

Spec. No. GJ
2B14
Type: 13 mm
316 bush

Flights: 46,542
Failure at
Hole 1

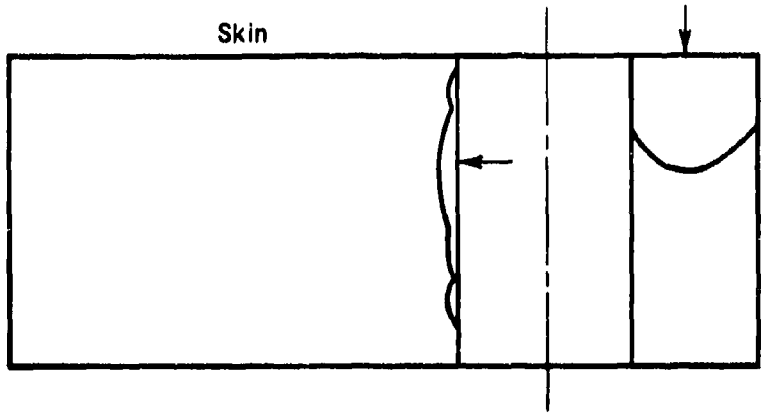

Spec. No. GJ
2A13
Type: 13 mm
304 bush

Flights: 57,100
Failure at
Hole 4

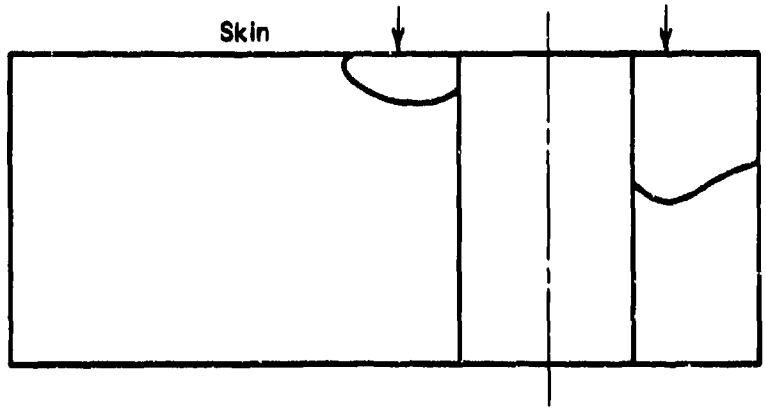

Spec. No. GJ
2B8
Type: 13 mm
304 bush

Flights: 67,142
Failure at
Hole 1

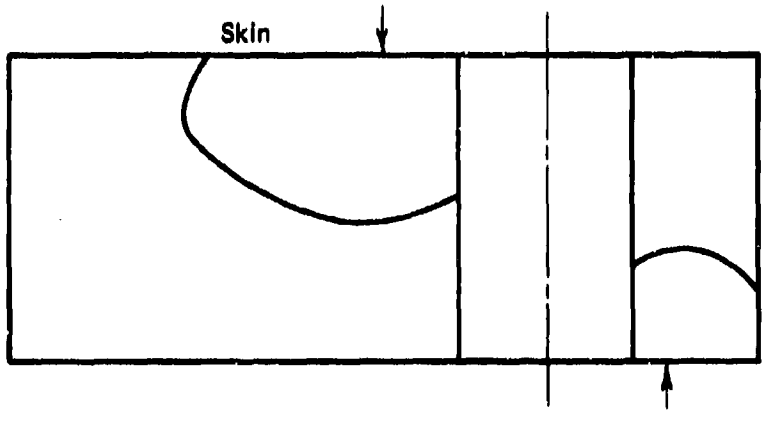

FIG. 14(I) FATIGUE-CRACKED AREAS

Spec. No. GJ
2B1
Type: refurbished
8.71 mm cold-expanded
Flights: 57,242
Failure at
Hole 1

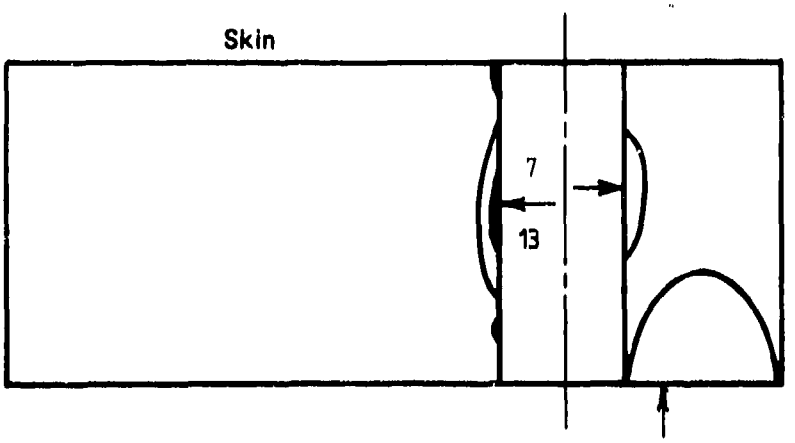

Spec. No. GJ
2A4
Type: refurbished
8.71 mm cold-expanded
Flights: 48,182
Failure at
Hole 1

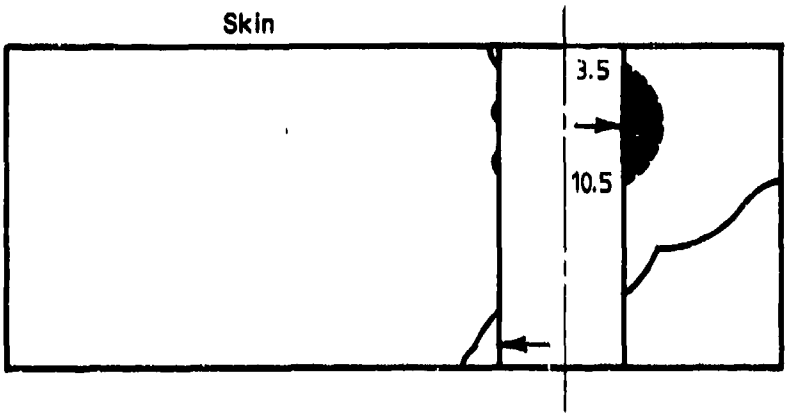

Spec. No. GJ
2B13
Type: refurbished
8.71 mm cold-expanded
Flights: 33,842
Failure at
Hole 5

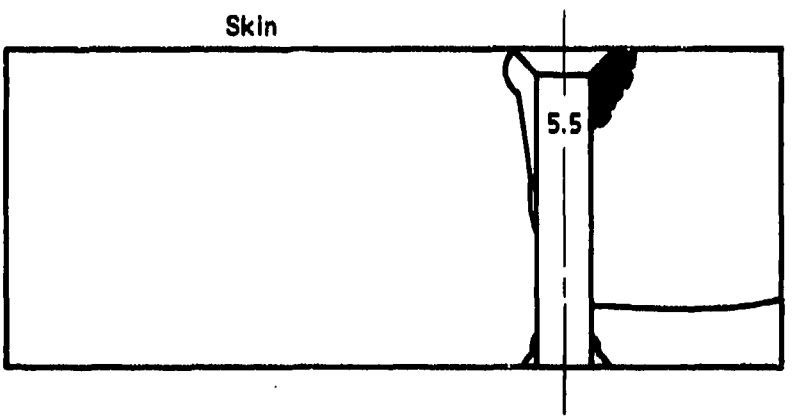

Dark shaded areas represent extent of residual fatigue cracking after refurbishment

FIG. 14(j) FATIGUE-CRACKED AREAS, REFURBISHED SPECIMENS

Spec. No. GJ
2A8
Type: refurbished
8.71 mm LAS
bush
Flights: 23,842
Failure at
Hole 4

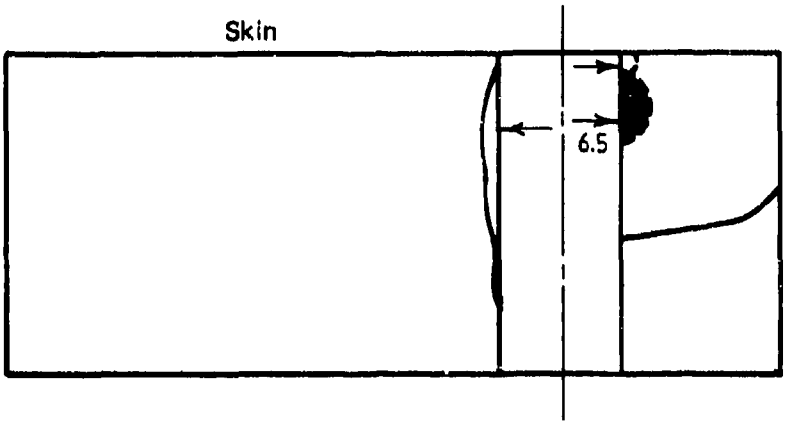

Spec. No. GJ
2B7
Type: refurbished
8.71 mm LAS
bush
Flights: 22,842
Failure at
Hole 1

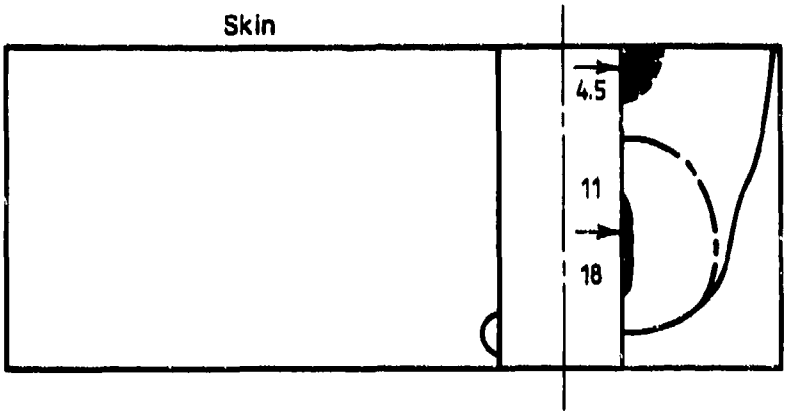

Spec. No. GJ
2A12
Type: refurbished
8.71 mm LAS
bush
Flights: 35,130
Failure at
Hole 1

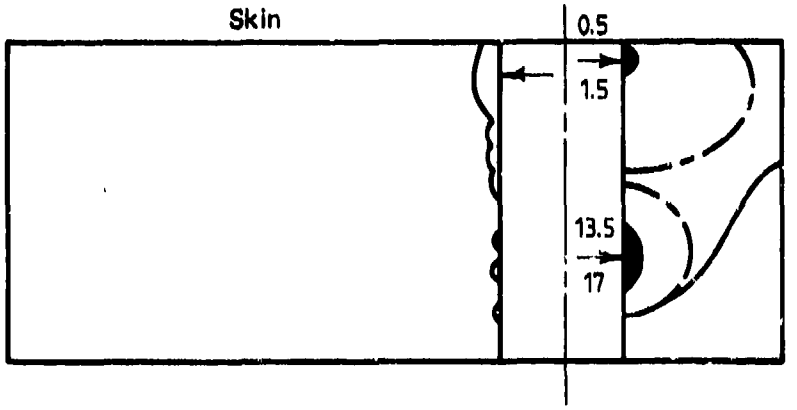

Dark shaded areas represent extent of residual fatigue cracking after refurbishment

FIG. 14(k) FATIGUE-CRACKED AREAS, REFURBISHED SPECIMENS

Skin

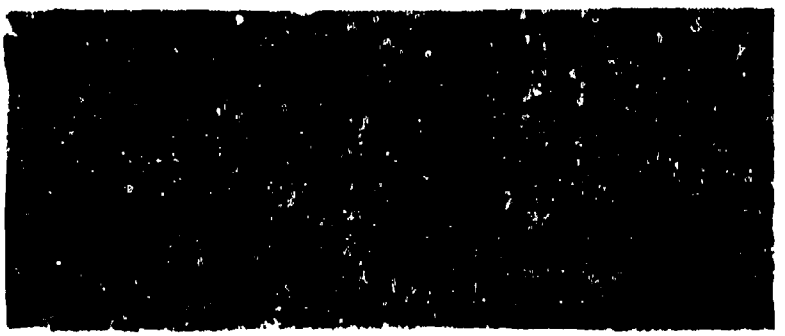

GJ1R
8 mm control
Failure hole 1
Flights 14,025

Skin

GJ1P
8 mm cold-expanded
Failure hole 4
Flights 48,642

Skin

GJ2B4
11 mm LAS bush
Failure hole 5
Flights 29,100

Skin

GJ2B3
11 mm LAS bush
Failure hole 4
Flights 44,462

FIG. 15(a) REPRESENTATIVE FATIGUE FRACTURE SURFACES

Skin

GJ2A9
11 mm 316 bush
Failure hole 1
Flights 57,580

Skin

GJ2A13
13 mm 304 bush
Failure hole 4
Flights 57,100

Skin

GJ2A4
Refurbished 8.71
mm cold-expanded
Failure hole 1
Flights (total)
48,182

Skin

GJ2A12
Refurbished 8.71
mm LAS bush
Failure hole 1
Flights (total)
35,130

FIG. 15(b) REPRESENTATIVE FATIGUE FRACTURE SURFACES

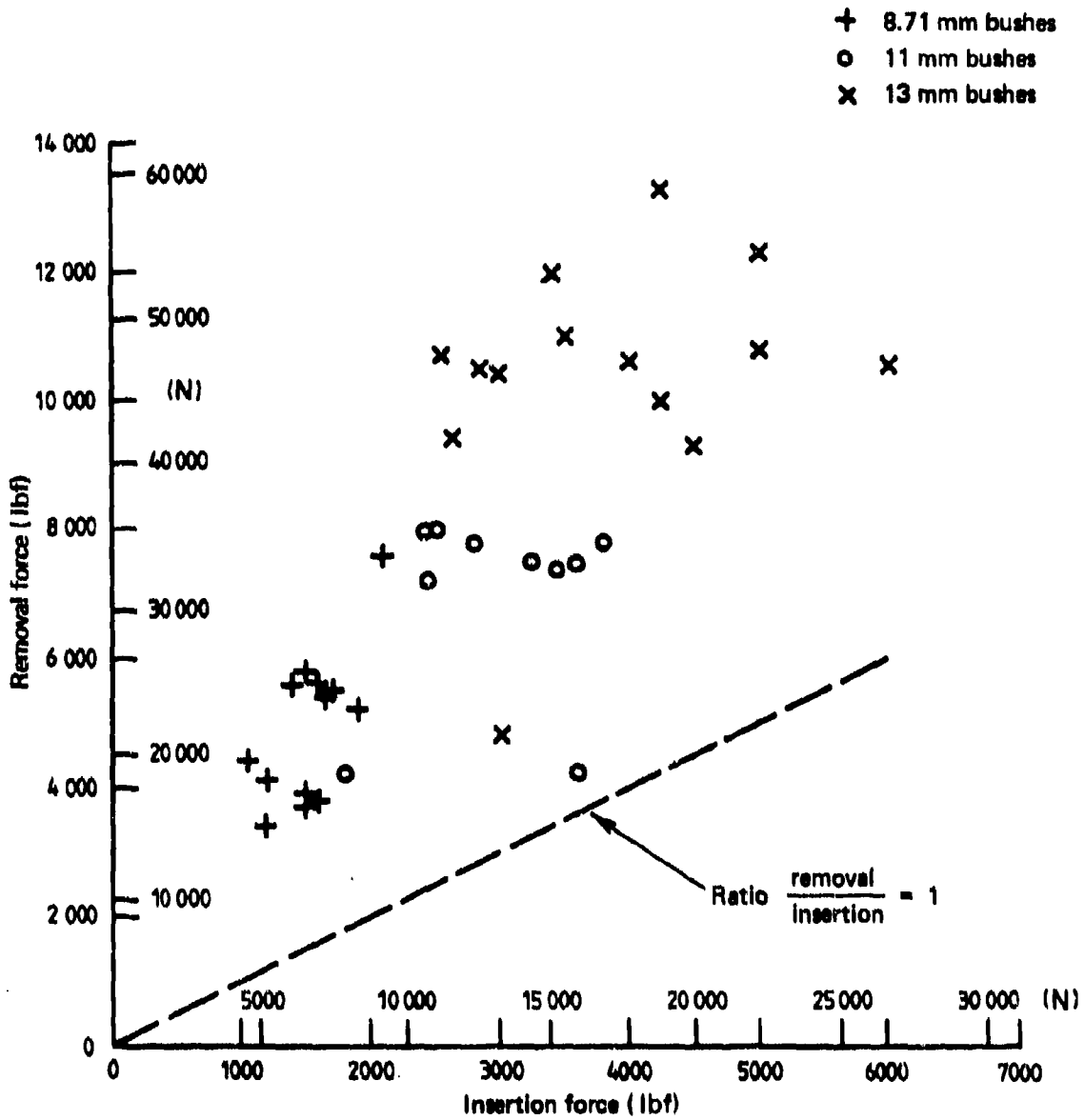

FIG. 16 BUSH INSERTION AND REMOVAL FORCES

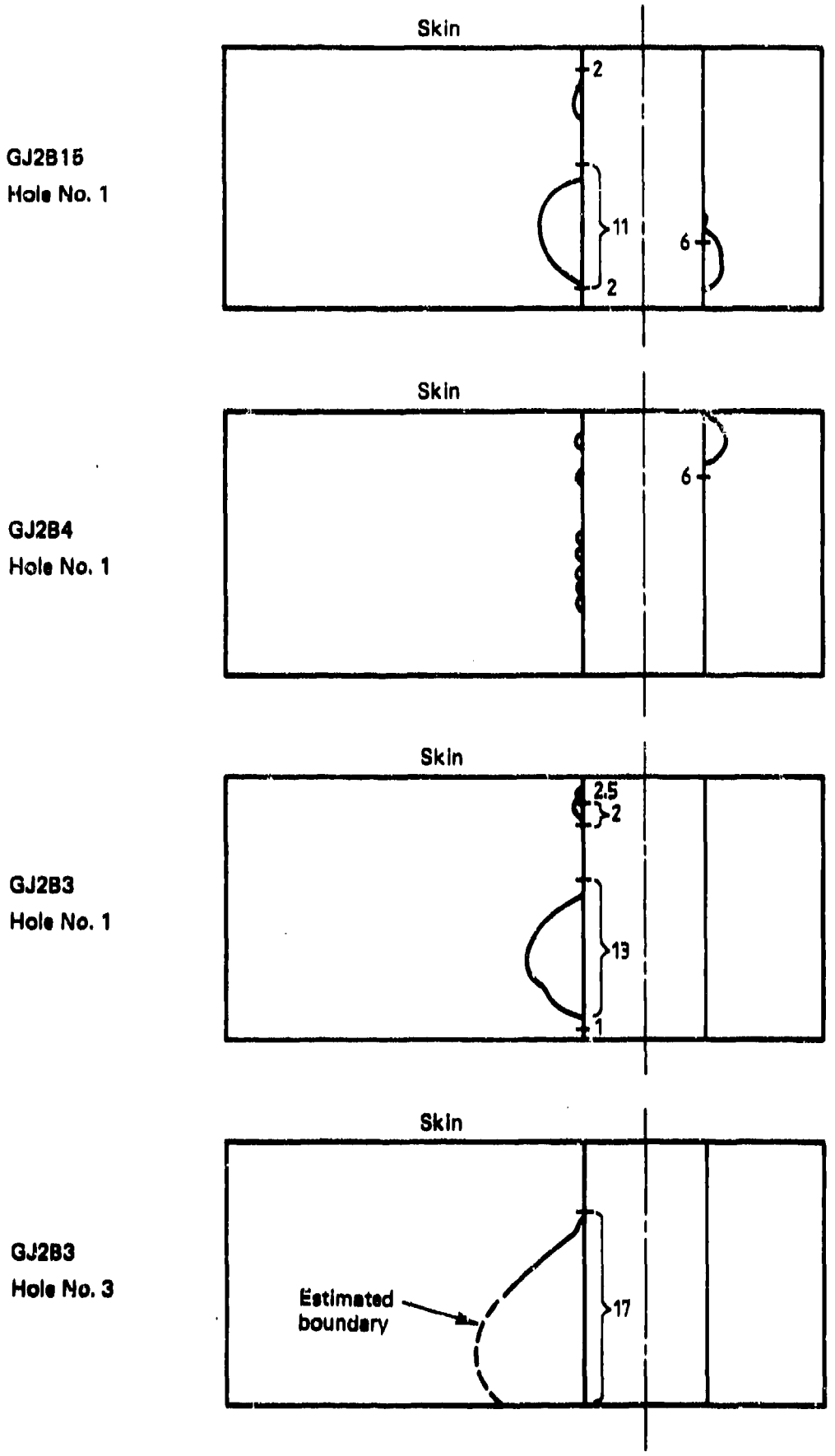

FIG. 17(a) COMPARISON OF FATIGUE-CRACKED AREAS WITH NDI ESTIMATES OF CRACK POSITIONS AND LENGTHS IN HOLES

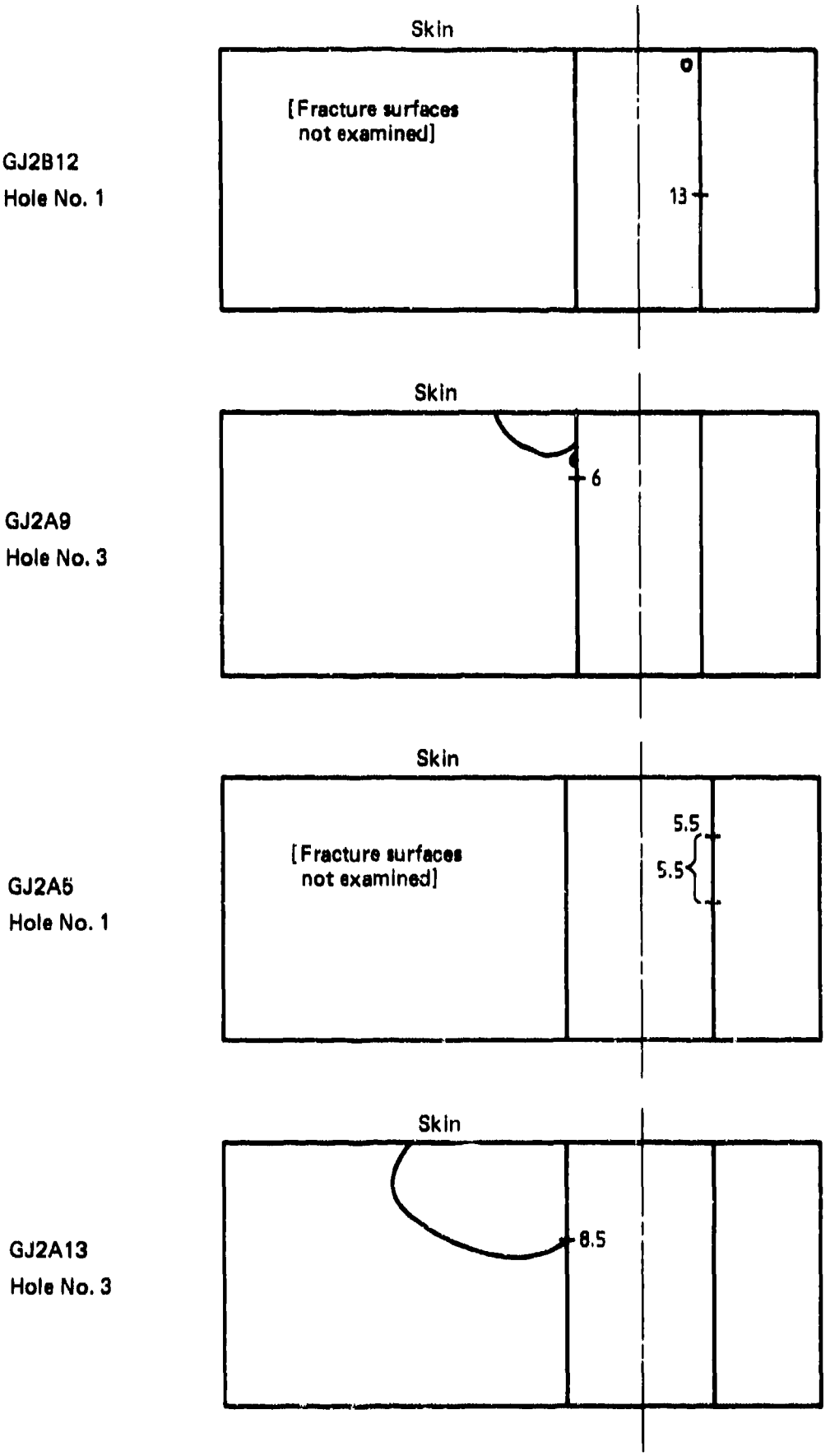

FIG. 17(b) COMPARISONS OF FATIGUE-CRACKED AREAS WITH NDI ESTIMATES OF CRACK POSITIONS AND LENGTHS IN HOLES

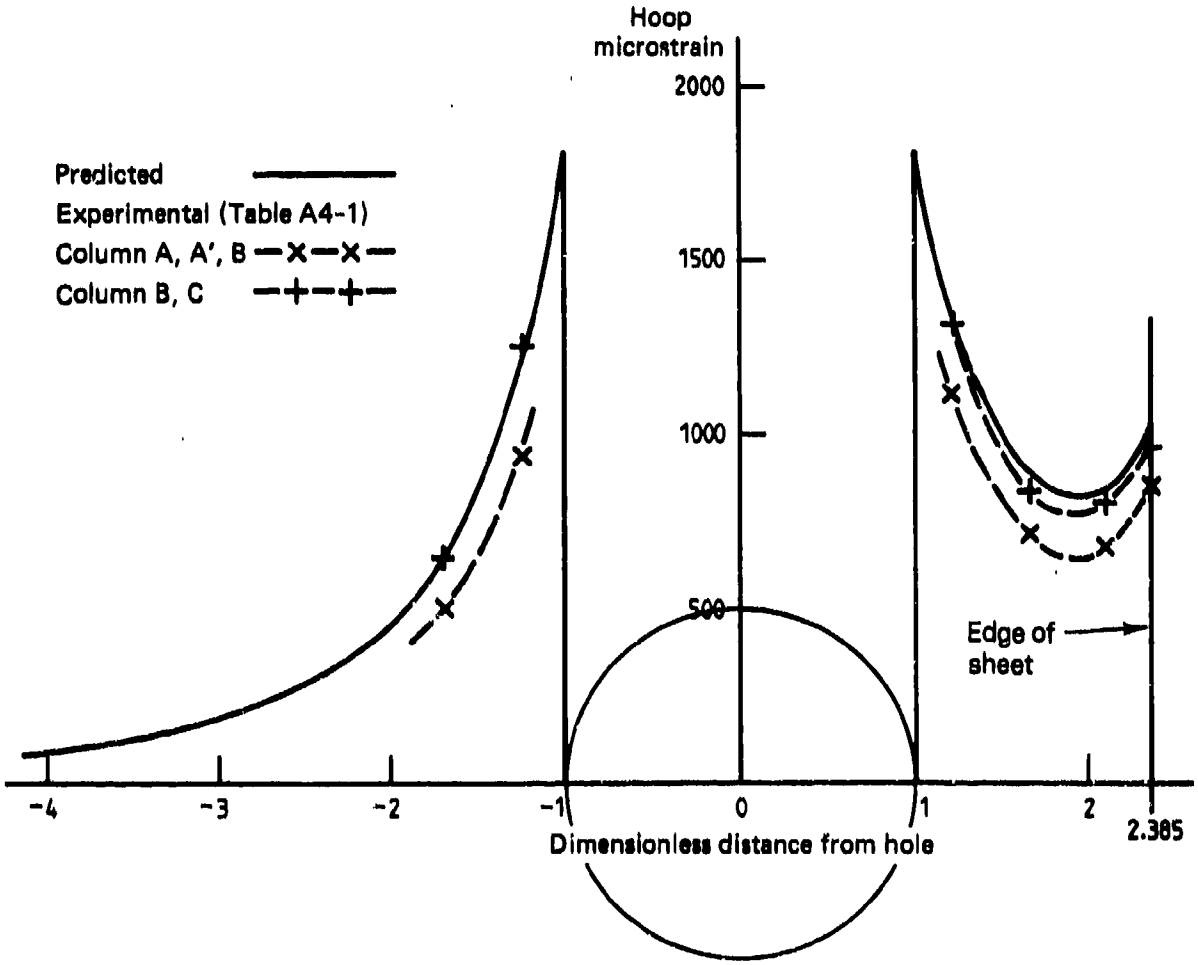

FIG. 18 PREDICTED PLANE STRAIN HOOP STRAIN DISTRIBUTION ALONG y AXIS (FIG A5-1) AND EXPERIMENTAL DATA POINTS (Appendix 4)

DISTRIBUTION

AUSTRALIA

DEPARTMENT OF DEFENCE

Central Office

Chief Defence Scientist
Deputy Chief Defence Scientist
Superintendent, Science and Technology Programmes
Controller, Projects and Analytical Studies
} 1 copy

Defence Science Representative (U.K.) (Doc. Data sheet only)
Counsellor, Defence Science (U.S.A.) (Doc. Data sheet only)
Defence Central Library
Document Exchange Centre, D.I.S.B. (17 copies)
Joint Intelligence Organisation
Librarian H Block, Victoria Barracks, Melbourne

Aeronautical Research Laboratories

Director
Library
Superintendent—Structures
Divisional File—Structures
Authors: J. Y. Mann
G. W. Revill
W. F. Lupsen
G. S. Jost
B. C. Hoskin
J. M. Finney
A. S. Machin

Materials Research Laboratories

Director/Library

Defence Research Centre

Library

Navy Office

Navy Scientific Adviser
Directorate of Naval Aircraft Engineering

Army Office

Army Scientific Adviser
Engineering Development Establishment, Library

Air Force Office

Air Force Scientific Adviser
Director General Aircraft Engineering—Air Force
HQ Support Command (SENGSO)

DEPARTMENT OF DEFENCE SUPPORT

Government Aircraft Factories
Manager
Library

DEPARTMENT OF AVIATION

Library
Flying Operations and Airworthiness Division,
Melbourne, Mr K. R. A. O'Brien
Canberra, Mr C. Torkington

STATUTORY & STATE AUTHORITIES AND INDUSTRY

Australian Atomic Energy Commission, Director
CSIRO
Materials Science Division, Library
Trans-Australia Airlines, Library
Qantas Airways Limited
SEC of Vic., Herman Research Laboratory, Library
Ansett Airlines of Australia, Library
B.H.P., Melbourne Research Laboratories
Commonwealth Aircraft Corporation
Library
Mr K. J. Kennedy (Manager Aircraft Factory No. 1)
Hawker de Havilland Aust. Pty. Ltd., Bankstown, Library

UNIVERSITIES AND COLLEGES

Adelaide	Barr Smith Library
Melbourne	Engineering Library
Monash	Hargrave Library
	Professor I. J. Polmear, Materials Engineering
Newcastle	Library
New England	Library
Sydney	Engineering Library
N.S.W.	Physical Sciencies Library
	Metallurgy Library
Queensland	Library
Tasmania	Engineering Library
Western Australia	Library
R.M.I.T.	Library

CANADA

CAARC Coordinator Structures
International Civil Aviation Organization, Library
Energy Mines & Resources Dept.
Physics and Metallurgy Research Laboratories

NRC
Aeronautical & Mechanical Engineering Library
Division of Mechanical Engineering, Director

Universities and Colleges

Toronto — Institute for Aerospace Studies

FRANCE

ONERA, Library

INDIA

CAARC Coordinator Structures
Defence Ministry, Aero Development Establishment, Library
Hindustan Aeronautics Ltd., Library
National Aeronautical Laboratory, Information Centre

INTERNATIONAL COMMITTEE ON AERONAUTICAL FATIGUE

per Australian ICAF Representative (25 copies)

ISRAEL

Technion—Israel Institute of Technology
Professor J. Singer
Professor A. Buch

JAPAN

National Research Institute for Metals, Fatigue Testing Division
Institute of Space and Astronautical Science, Library

Universities

Kagawa University — Professor H. Ishikawa

NETHERLANDS

National Aerospace Laboratory (NLR), Library

Universities

Technological University of Delft — Professor J. Schijve

NEW ZEALAND

Defence Scientific Establishment, Library
RNZAF, Vice Consul (Defence Liason)

Universities

Canterbury — Library
Professor D. Stevenson, Mechanical Engineering

SWEDEN

Aeronautical Research Institute, Library
Swedish National Defence Research Institute (FOA)

SWITZERLAND

Armament Technology and Procurement Group
F+W (Swiss Federal Aircraft Factory)

UNITED KINGDOM

Ministry of Defence, Research, Materials and Collaboration
CAARC, Secretary (NPL)
Royal Aircraft Establishment
  Bedford, Library
  Farnborough, Library
Commonwealth Air Transport Council Secretariat
Admiralty Marine Technology Establishment, Library
National Gas Turbine Establishment
  Director, Pyestock North
National Physical Laboratory, Library
National Engineering Laboratory, Library
British Library, Lending Division
CAARC Coordinator, Structures
Fulmer Research Institute Ltd., Research Director
Motor Industry Research Association, Director
Rolls-Royce Ltd.
  Aero Division Bristol, Library
Welding Institute, Library
British Aerospace
  Hatfield-Chester Division, Library
British Hovercraft Corporation Ltd., Library
Short Brothers Ltd., Technical Library

Universities and Colleges

Bristol	Engineering Library
Nottingham	Science Library
Southampton	Library
Strathclyde	Library
Cranfield Institute of Technology	Library
Imperial College	Aeronautics Library

UNITED STATES OF AMERICA

NASA Scientific and Technical Information Facility
Applied Mechanics Reviews
Metals Information
The John Crerar Library
The Chemical Abstracts Service
Boeing Co.
  Mr R. Watson
  Mr J. C. McMillan
Lockheed-California Company
Lockheed Georgia
McDonnell Aircraft Company, Library
Nondestructive Testing Information Analysis Center

Universities and Colleges	
Iowa	Professor R. I. Stephens
Illinois	Professor D. C. Drucker
Massachusetts Inst. of Technology	M.I.T. Libraries

SPARES (15 copies)

TOTAL (178 copies)

Department of Defence

DOCUMENT CONTROL DATA

1. a. AR No.	1. b. Establishment No.	2. Document Date	3. Task No.
AR-002-948	ARL-STRUC-NOTE-486	April, 1983	DST 79/130

4. Title	5. Security	6. No. Pages
IMPROVING THE FATIGUE PERFORMANCE OF THICK ALUMINIUM ALLOY BOLTED JOINTS BY HOLE COLD-EXPANSION AND THE USE OF INTERFERENCE-FIT STEEL BUSHES	a. document: Unclassified b. title: U. c. abstract: U.	36 7. No. Refs 36

8. Author(s)	9. Downgrading Instructions
J. Y. Mann, G. W. Revill and W. F. Lupson	—

10. Corporate Author and Address	11. Authority (*as appropriate*)
Aeronautical Research Laboratories, P.O. Box 4331, Melbourne, Vic. 3001.	a. Sponsor c. Downgrading b. Security d. Approval —

12. Secondary Distribution (*of this document*

Approved for public release.

Overseas enquirers outside stated limitations should be referred through ASDIS, Defence Information Services Branch, Department of Defence, Campbell Park, CANBERRA, ACT, 2601.

13. a. This document may be ANNOUNCED in catalogues and awareness services available to . . .

No limitations.

13. b. Citation for other purposes (*i.e. casual announcement*) may be (~~select~~) unrestricted (~~or) as for 13 a.~~

14. Descriptors		15. COSATI Group
Fatigue (materials)	Elastoplasticity	1113
Bolted joints	Fasteners (interference)	1103
Holes (openings)	Interference fitting	
Stress analysis	Bushings	
Cold working		
Aircraft structures		

16. Abstract

Fatigue tests under a flight-by-flight loading sequence have been carried out on small bolted joint specimens of 23 mm thickness representing part of the spar rear flange/skin attachment in Mirage III aircraft.

The investigation has shown that by cold-expanding the bolt holes to take standard oversize bolts, or by installing interference-fit bushes, the fatigue life can be more than doubled compared with the use of standard close-fit bolts in reamed holes. No significant differences were found between the fatigue lives of specimens embodying low-alloy steel or stainless steel bushes.

When small-sized residual fatigue cracks are present, hole cold-expansion may be a suitable process for extending the fatigue life. The use of interference-fit bushes is not likely to be an effective method for extending the fatigue lives when large-size residual cracks are present. However, if

This page is to be used to record information which is required by the Establishment for its own use but which will not be added to the DISTIS data base unless specifically requested.

16. Abstract (Contd

such cracks can be machined out, the incorporation of large-size interference-fit bushes has the greater potential for providing not only significant extensions in life but also significantly longer lives than the original design detail.

17. Imprint

Aeronautical Research Laboratories, Melbourne.

18. Document Series and Number	19. Cost Code	20. Type of Report and Period Covered
Structures Note 486	25 1020	—

21. Computer Programs Used

—

22. Establishment File Ref(s)

—